Geoarchaeology

ARCA

February 2022

Report Number: 2122-2

SHINFIELD STUDIOS, CUTBUSH LANE EAST, SHINFIELD, READING: GEOARCHAEOLOGICAL BOREHOLE STUDY

Prepared for Cotswold Archaeology

Keith Wilkinson, Rob Batchelor and Phil Toms

ARCA
Department of Archaeology, Anthropology and Geography
University of Winchester
Winchester
SO22 4NR
http://www.arcauk.com

Vers.	Date	Status*	Prepared by	Author's signature	Approved by	Approver's Signature
001	03/02/2022	I	Keith Wilkinson		?	
*I – Internal draft; E – External draft; F – Final						

CONTENTS

FIGURES

TABLES

SUMMARY

A geoarchaeological borehole study was undertaken of land west of Cutbush Lane East, Shinfield, Reading in October 2021, while subsequent laboratory examination took place from October 2021 to February 2022. The purpose of the work was to test the Palaeolithic archaeological potential of deposits on the site that had been revealed by a previous archaeological evaluation.

Six geoarchaeological boreholes were drilled, four with an Atlas Cobra TT hammer driving gouge auger heads and core samplers, and two with a Pioneer 2 rig collecting 115mm diameter core samples. Strata in the gouge auger heads were described in the field, while cores were described and sub-sampled in the laboratory for optically stimulated luminescence (OSL) and ^{14}C dating, and palynological and plant macrofossil assessment.

Between 4 and 5m of Quaternary (the last 2.6 million years) deposits were found overlying London Clay (Eocene) bedrock. The basal Quaternary deposits are 1.1–1.5m thick fluvial gravel strata that probably formed in the bed of the Loddon river, a south bank tributary of the Thames. Two OSL dates from sand layers within the gravels suggest deposition in Marine Isotope Stage (MIS) 3 (29–57,000 years ago) and possibly MIS 4 (71,000–82,000 years ago). Overlying the gravel in one part of the site is a c 0.4m-thick organic mud, which is also thought to be of MIS 3 age. This latter deposit contains moderate to well preserved pollen, which was mostly of aquatic and herbaceous taxa, but also included possible evidence for trees. Plant macrofossils were not, however, found in the stratum meaning that it could not be chronometrically dated by ^{14}C measurement. Lying above the gravels and organic mud, and likely separated from them by a hiatus are 3–4m of Brickearth and Head deposits. The brickearths formed first, but later interdigitate and are therefore contemporary with the Head. While both are likely to be of MIS 2 age (11.7–29.0 thousand years ago).

The organic muds are assessed as being of moderate to high Palaeolithic archaeological potential on account of their age, gentle mode of deposition, the presence of a former land surface in one record and the moderate–good pollen preservation. The remaining deposits are assessed as either low to moderate (fluvial gravels) on account of their high energy deposition or low potential (Brickearth and Head) because of their chronology and the absence of humans for the majority of MIS 2.

1. INTRODUCTION

1.1 This document reports the results of a geoarchaeological study carried out on land to the west of Cutbush Lane East, Shinfield, Reading (henceforth 'the site'). The work was carried out as set out in a Written Scheme of Investigation (WSI) (Wilkinson 2021), and in accordance with Historic England's (2015) guidance on geoarchaeology, environmental archaeology (Campbell et al. 2011) and the Chartered Institute for Archaeologist's (CIfA) (2014) *Standards and guidance for archaeological field evaluation*. ARCA undertook the project on behalf of Cotswold Archaeology and their client, Shinfield Studios Ltd, the latter organisation proposing to develop the site as a Science Park Creative Media Hub that would comprise workshops, offices, film stages and associated infrastructure

1.2 The site lies south of Reading, is centred on NGR SZ 50590 88400, ranges between +65 (in the north-west) to +40m OD (in the south-east) and comprises an area of 22.5 ha (Figure 1A and 1B). ARCA's fieldwork took place on 13–15 October 2021 at which time the single field that was investigated comprised scrub (Figure 1C). This latter vegetation had developed since a prior archaeological evaluation of the land by Wessex Archaeology (WA) in March 2021 (Dawkins et al. 2021). However, before spring 2021 the land had been used for arable cultivation.

1.3 As reported in the WSI (Wilkinson 2021), The British Geological Survey (BGS) map the bedrock geology of the study area as deposits of London Clay Formation, an Eocene unit (of Ypresian Age) dating between 56 and 48 million years ago (British Geological Survey 2021a, 2021b). The BGS also map superficial Brickearth strata overlying London Clay in the eastern and River Terrace Deposits 2 (the latter of the Blackwater-Loddon catchment) in the southern part of the study area.

1.4 The work described in this report is the result of recommendations made in the WA archaeological evaluation report (Dawkins et al. 2021). The latter comprised 90 evaluation trenches and 20 geoarchaeological test pits. Post-medieval ditches of low archaeological significance were found by the evaluation in the northern and central part of the study area. However, two of the geoarchaeological test pits (TP1400 and TP1600) encountered potentially important strata (see Figure 1C). These latter comprised organic clays and which overlay sands and gravels of River Terrace Deposits 2 and were capped by Brickearth. The stratigraphic position of the organic deposits suggested a Pleistocene age, while apparently good plant macrofossil preservation indicated a possible Palaeolithic archaeological significance (Dawkins et al. 2021).

1.5 The present geoarchaeological investigation has therefore been carried out to determine the archaeological and palaeoenvironmental potential of potential Pleistocene deposits in the area of WA TP1400 and TP1600. Therefore, while the extent of the site is as described in Sections 1.1–1.4 above, the present investigation was only of that part extending 200m northwards from an unpaved track (Pearmans Lane) and 40m west of Cutbush Lane East (Figure 1C).

1.6 The aims of the present geoarchaeological study were set out in the WSI (Wilkinson 2021) and are in accordance with priorities established in the Lower/Middle Palaeolithic research agenda of the *Solent-Thames Research Framework for the Historic Environment* (Wenban-Smith et al. 2014). They are to:

1.6.1 Characterise the Quaternary lithostratigraphy of the central part of the study area;

1.6.2 Determine the mode of formation of Quaternary strata within the study area (Wenban-Smith et al. 2014 section 4.6.4);

1.6.3 Provide a chronology for the Pleistocene strata (Wenban-Smith et al. 2014 sections 4.6.3 and 4.6.5);
1.6.4 Assess the preservation of biological palaeoenvironmental proxies;
1.6.5 Determine the likelihood of *in situ* Palaeolithic archaeological preservation (Wenban-Smith et al. 2014 section 4.6.9);

And by resolving the Aims 1.6.1–1.6.5 to:

1.6.6 Assess the Palaeolithic archaeological potential of the site.

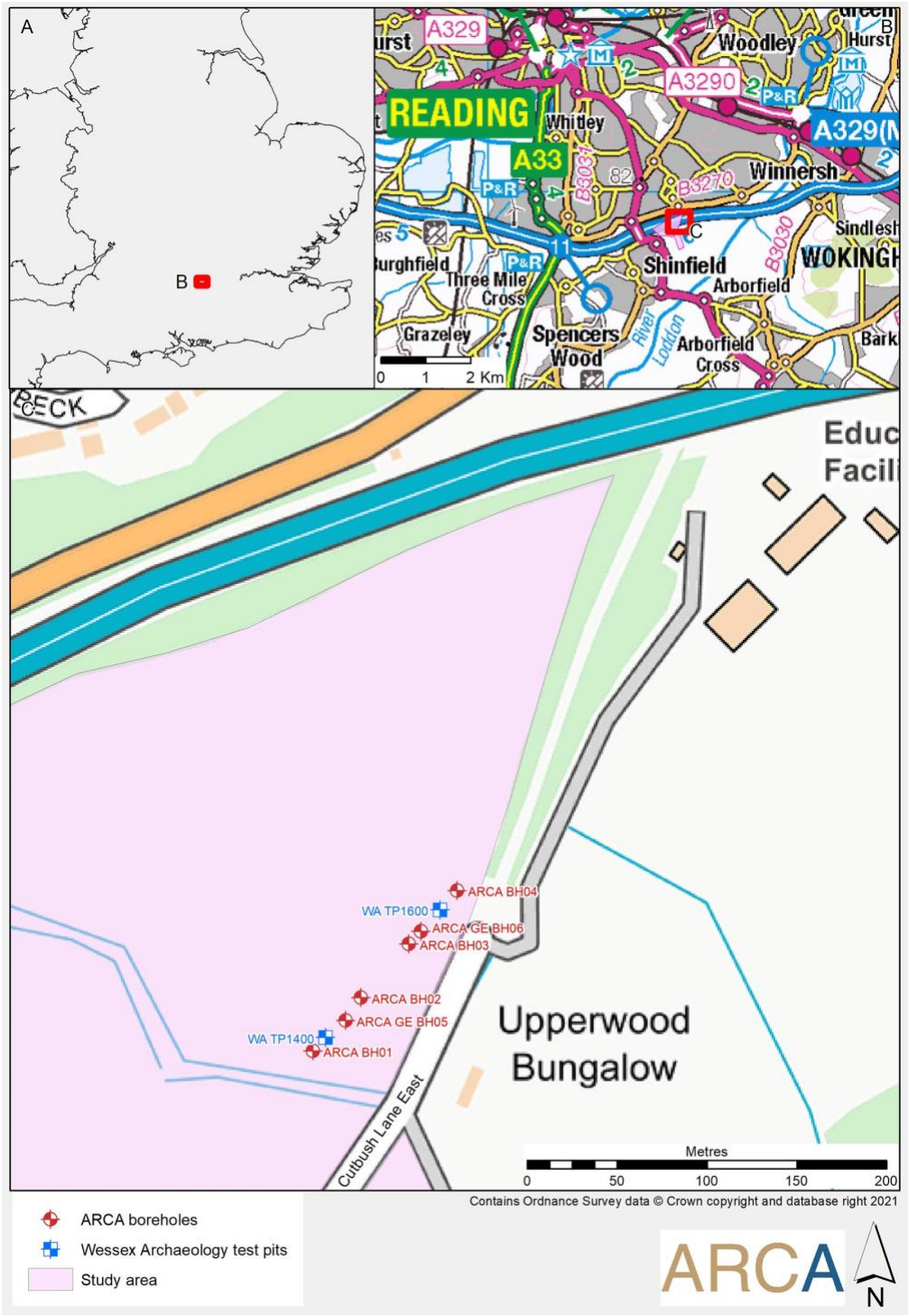

Figure 1. Location of study area within (A) southern England and (B) Reading, and (C) position of ARCA boreholes and select Wessex Archaeology test pits within the site

1.7 The remaining sections of this report first set out the methodologies by which the geoarchaeological study at Cutbush Lane East was carried out. The strata revealed in the boreholes are then described and interpreted (Aims 1.6.1–1.6.2) after which the results of bioarchaeological assessment and optically stimulated luminescence are discussed (Aims 1.6.3–1.6.4). Finally, the Assessment section considers whether Palaeolithic archaeological remains might exist on the site and thus the nature of Palaeolithic archaeological potential (Aims 1.6.5–1.6.6).

2. METHODOLOGY

2.1 Fieldwork

2.1.1 The methodology employed in the field and subsequently was that described in the WSI (Wilkinson 2021, section 2).

2.1.2 A total of six boreholes were drilled in the locations shown in Figure 1c. Four of the boreholes were advanced using an Atlas Cobra TT petrol-powered hammer driving Eijkelkamp gouge and core sampling heads (ARCA BH01–BH04), while two were drilled with a a Pioneer 2 dynamic probe geotechnical rig (ARCA GE BH05–BH06). The Atlas Cobra TT/Eijkelkamp borehole locations were planned in an ArcGIS 10.4 project prior to the fieldwork and were positioned so as to infill and extend a transect linking WA TP1400 and WA TP1600. The positional data were uploaded from ArcGIS to a Leica GS16 RTK GPS and the latter device used to locate the drilling positions in the field. The positions of the Pioneer 2 boreholes were decided on the basis of stratigraphy revealed in the Atlas Cobra TT/Eijkelkamp boreholes. All borehole positions were re-surveyed using the Leica GS16 RTK GPS and these latter locations uploaded to RockWorks 17 (Appendix 1).

2.1.3 Atlas Cobra/Eijkelkamp boreholes were drilled from the ground surface to a maximum depth of 5m below ground level or the top of strata of River Terrace Deposits 2, whichever occurred first. Gouge auger heads of 75–60mm diameter and 1000mm length were employed, and the strata so-recovered photographed (Appendix 3) and described using standard geological criteria in the field (Appendix 2) (Jones *et al*. 1999, Munsell Color 2000, Tucker 2011). Cores of 50mm diameter and 1000m length were, however, recovered from depths in ARCA BH01 and ARCA BH04 thought to correspond to the organic clays described in WA TP1400 and WA TP1600. These cores were labelled and sealed, and then transported to ARCA's Winchester laboratory for detailed study. All four Atlas Cobra/Eijkelkamp boreholes were then backfilled with the arisings as extracted from the gouge auger heads.

2.1.4 The Pioneer 2 drilling rig was operated by a crew from Geotechnical Engineering Ltd. At ARCA GE BH05 and ARCA GE BH06 a 1.2m-deep inspection pit of 200mm diameter was first excavated with pincers to check for buried services. Casing was then inserted and the boreholes were advanced by percussive means in 1.5m-long increments and employing a 100mm diameter core sampler. Cores were labelled and sealed, and transported to Geotechnical Engineering's Gloucester warehouse for further study. The Pioneer 2 boreholes were backfilled with inert bentonite pellets.

2.1.5 Upon completion of fieldwork, lithological (i.e. field descriptions of strata sampled in the gouge auger heads) and positional (downloaded from the Leica GS16) data were transferred into a RockWorks 17 database that also contained lithostratigraphic data from WA TP1400 and WA TP1600 as transcribed from WA's archaeological evaluation report (Dawkins et al. 2021).

2.2 Laboratory core description and sub-sampling

2.2.1 In either ARCA's Winchester laboratory (ARCA BH01 and ARCA BH04) or Geotechnical Engineering's Gloucester warehouse (ARCA GE BH05 and ARCA GE BH06), the plastic sleeves containing the borehole cores were cut open with a hooked knife blade. A c. 1mm-thick sliver of the sediment so-exposed was then removed with a scalpel, and the core photographed and described using the same geological criteria as employed in the field (Jones *et al*. 1999, Munsell Color 2000, Tucker 2011).

Figure 2. OSL sampling of ARCA GEBH05 (top – 1.00m on scale = 5.00m bgl) and ARCA GEBH06 (bottom – 1.00m on scale = 4.00m bgl)

Table 1. Samples collected from the Cutbush Lane East boreholes

Bore	Top[1]	Base[1]	Purpose	Measured/assessed?
ARCA BH04	4.44	4.45	Pollen	
ARCA GE BH05	4.50	4.51	Pollen	
ARCA GE BH05	4.56	4.57	Pollen	
ARCA GE BH05	4.63	4.64	Pollen	
ARCA GE BH05	4.71	4.72	Pollen	
ARCA GE BH05	4.72	4.77	Plant macros	Assessed
ARCA GE BH05	4.79	4.80	Pollen	
ARCA GE BH05	4.87	4.88	Pollen	
ARCA GE BH05	4.88	4.93	Plant macros	Assessed
ARCA GE BH05	4.95	4.96	Pollen	
ARCA GE BH05	5.44	5.51	OSL1	Measured
ARCA GE BH05	5.46	5.47	Pollen	
ARCA GE BH06	4.07	4.14	OSL2	Measured

[1] m bgl

2.2.4 Two bulk sediment sub-samples each comprising a block of sediment measuring 50mm (top to bottom) and 50mm thickness (into the core) were taken from organic silt/clay strata in ARCA GE BH05 (Table 1). Both sub-samples were submitted to Dr Rob Batchelor of Quest for plant macroremain assessment. Dr Batchelor was also asked to extract terrestrial plant macrofossils that might be used for AMS ^{14}C dating, but no such remains were encountered.

2.2.3 Nine sub-samples each of 4ml were taken using a volumetric sampler through organic silt/clay strata underlying the brickearth and silt/clay lenses within gravels of River terrace deposits 2 in ARCA BH04 and ARCA GE BH05 (Table 1). Six such sub-samples were sent to Dr Batchelor for palynological assessment.

2.2.2 Sub-samples were taken from ARCA GE BH05 and ARCA GE BH06 for optically stimulated luminescence (OSL) dating by inserting a 55mm-diameter by 100mm-long tube in available sand lenses within the gravels of River terrace deposits 2 (Figure 2). The upper end of the tube was sealed using multiple layers of black duct tape, removed from the core and the lower end similarly sealed to prevent light ingress. The two samples so taken were sent to Prof Phil Toms of the Luminescence Dating Laboratory, University of Gloucestershire for OSL measurement (Table 1).

2.3 Optically stimulated luminescence

2.3.1 The methodology employed by the University of Gloucestershire in processing and measuring luminescence of the two samples submitted, and then calculating their age is described in detail in Appendix 4. Appendix 4 also explains the assumptions that have been made in age calculation and potential causes of error.

2.4 Palynology

2.4.1 Six subsamples from ARCA GE BH05 were extracted for an assessment of pollen content (Table 1). The pollen was extracted as follows: (1) sampling a standard volume of sediment (1ml); (2) deflocculation of the sample in 1% Sodium pyrophosphate; (3) sieving of the sample to remove coarse mineral and organic fractions (>125µm); (4) acetolysis; (5) removal of finer minerogenic fraction using Sodium polytungstate (specific gravity of 2.0g/cm^3); (6) mounting of the sample in glycerol jelly. Each stage of the procedure was preceded and followed by thorough sample cleaning in filtered distilled water. Quality control is maintained by periodic checking of residues, and assembling sample batches from various depths to test for systematic laboratory effects. Pollen grains and spores were identified using the University of Reading pollen type collection and the following sources of keys and photographs: Moore *et al* (1991); Reille (1992). The assessment procedure consisted of scanning the prepared slides, and recording the concentration and preservation of pollen grains and spores, and the principal taxa on four transects (10% of the slide) (Table 4).

2.5 Plant macro remains

2.5.1 Two bulk samples from ARCA GE BH05 were assessed for the presence and concentration of macrofossil remains, including waterlogged and charred plant macrofossils, wood, insects and Mollusca. The samples were scanned under a stereozoom microscope at x7-45 magnification, and sorted into the different macrofossil classes.

2.6 Archive

2.6.1 The Pioneer 2 borehole cores were discarded immediately following photography, description and sub-sampling, while the remaining material archive comprises the samples listed in Table 2.

2.6.2 The digital archive comprises a RockWorks 17 (SQLite) database housing the positional and stratigraphic data, photographs of the borehole cores as image files (compressed TIF format) and Excel spreadsheets holding the palynological and plant macrofossil assessment data. These data will be held in perpetuity at the University of

Winchester (RockWorks, images) and University of Reading (Excel), while exported versions of the data are included in this report as Appendices 1–5).

Table 2. Material archive, location and discard policy

Type	Number	Location	Discard policy[2]
50mm x 1000mm diameter cores from ARCA BH01 and ARCA BH06	4	University of Winchester	Will be disposed of on 14 October 2022
4ml palynological sub-samples (unprocessed)	3	University of Winchester	Will be disposed of on 14 October 2022
Slides prepared from processed pollen samples	6	University of Reading	

[2] Unless requested otherwise (a retention fee will apply)

3. LITHOSTRATIGRAPHY

3.0.1 Deposits revealed in the six ARCA boreholes and WA TP1400 and TP1600 are plotted as a composite cross section (Figure 3), while detailed lithostratigraphic descriptions and photographs of sediment retained in the gouge auger heads and cores are provided in Appendix 2 and 3 respectively. The following text synthesises the depositional sequence in reverse stratigraphic order.

3.1 London Clay Formation

3.1.1 Dark grey (Munsell 5 Y 4/1) compact silt/clay was observed in ARCA GE BH05 and ARCA GE BH06 at 5.67–6.15m bgl (+39.69–+39.21m OD). However, the remaining ARCA boreholes and WA TP1400 and TP1600 did not penetrate the overlying gravels (see Section 3.2).

3.1.2 These silt/clays are the London Clay Formation, which as described in Section 1.3 is of Eocene age and the bedrock geology of the study area.

3.2 'River Terrace 2'

3.2.1 Sand and gravel strata unconformably overlie the London Clay Formation in ARCA BH05 and ARCA BH06, and also sub-crop in all other ARCA boreholes and WA test above 6.15m bgl (+39.21m OD). The upper contact of the unit is at variable depths/elevations ranging from 5.03m bgl (+40.36m OD) in ARCA GE BH05 to 3.36m bgl (+42.00m OD) in ARCA BH03. Indeed, the composite cross section suggests that the upper surfaces of the sands and gravels undulates and that two depressions occur, one centred on ARCA GE BH05 and the other on WA TP1600.

3.2.2 The sand and gravel strata are best represented in ARCA GE BH05 and ARCA GE BH06 where their entire thickness has been described. In these boreholes the unit is composed of 50–100mm thick sets of sub-rounded pebble and granular sized flint in a coarse sand matrix. Interbedded strata of c 110–80mm thickness and comprising moderately sorted coarse and medium sands and fine sands and silts are also recorded (these are the deposits sampled for OSL dating – see Section 4).

3.2.3 The sands and gravels are the strata mapped by the BGS as River terrace deposits 2 (Section 1.3), and which were deposited on top of strata of the London Clay Formation following considerable weathering and erosion of the latter. The irregular nature of the upper contact of the sands and gravels in turn suggests weathering, while the depressions are likely the result of channel development.

3.3 Organic mud

3.3.1 Dark grey (5 Y 4/1) and very dark grey (2.5 Y 3/1) organic silt/clays unconformably overlie the sands and gravels within the two depressions in WA TP1400, ARCA GE BH05, ARCA BH02 and WA TP1600. The organic mud varies in thickness between 470mm (ARCA BH GE05) and 170mm (WA TP1600), while the stratum is both thicker and more extensive (occupying at least a 32m width of the section) in the eastern depression than the western (where it was described only in WA TP1600) (Figure 3).

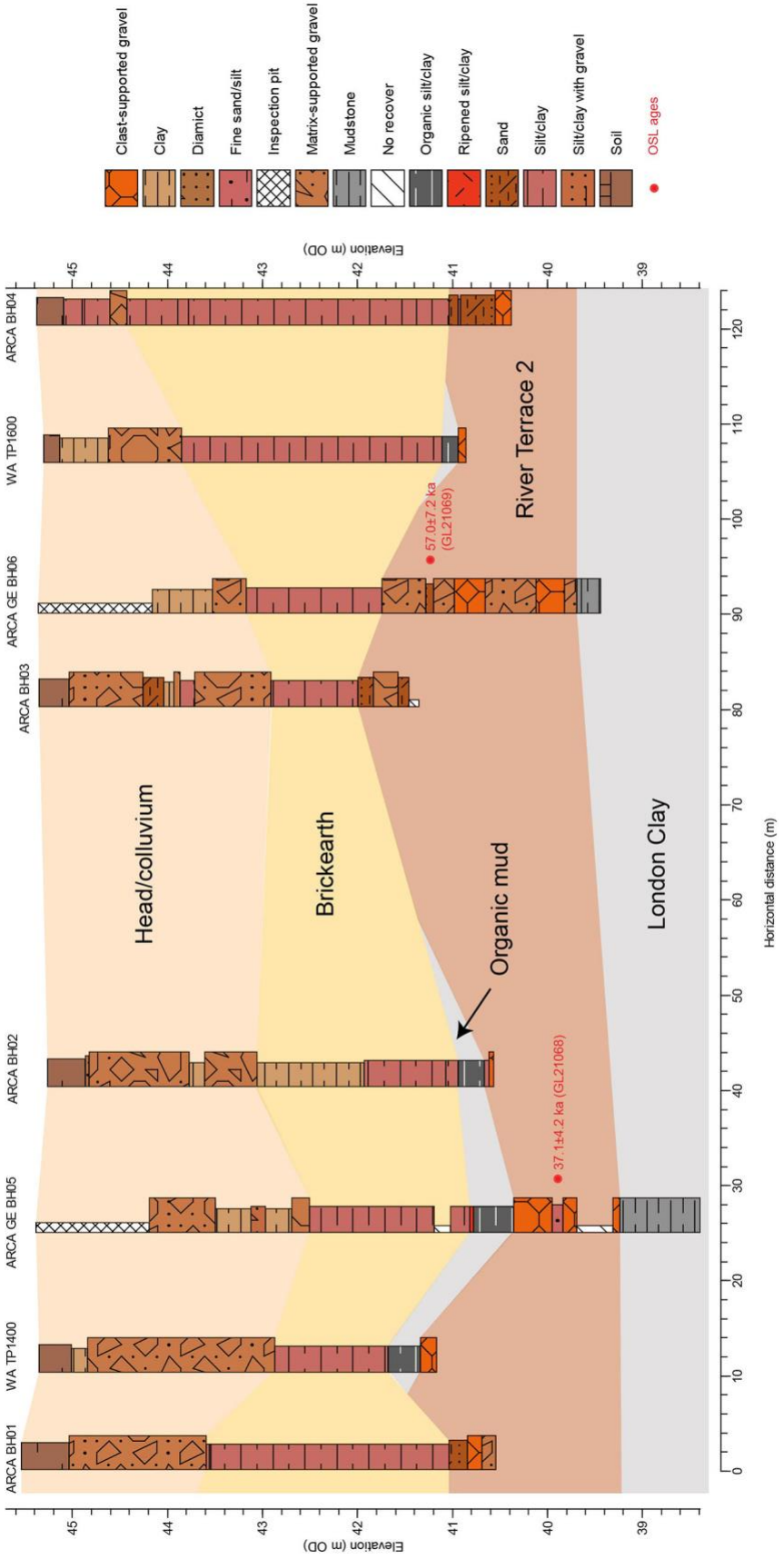

Figure 3. East–west composite cross section through the Cutbush Lane East site

3.3.2 Although described in both the field and laboratory as 'organic', the stratum contained no discernible plant macro remains other than occasional fibres, and rather the presence of botanical remains was as finely divided material. In ARCA BH02 and probably in WA TP1400 and WA TP1600 too, the organic mud was homogeneous. However, in ARCA GE BH05 the upper 40mm of the unit is a couplet of a brown (7.5 YR 4/2) overlain by a dark greyish brown silt/clay (2.5 Y 4/2), the latter of a lighter colour than the main body of the organic mud (5 Y 4/1).

3.3.3 As is described in Section 1.4, the organic muds subcropping in WA TP1400 and WA TP1600 were the main reason for undertaking the present geoarchaeological works. It would appear that they and correlative deposits in ARCA GE TP05 and ARCA BH02 are low energy fills of channels cut in the top of the underlying sands and gravels. It is possible that the organic mud stratum is itself truncated at its surface in all records except ARCA GE BH05, while in the latter the lighter coloured layer and the underlying brown stratum are suggestive of weathering, ripening and hence soil formation.

3.4 'Brickearth'

3.4.1 Grey (2.5 Y 6/1) oxidising on exposure to air to strong brown (7.5 YR 4/6) silts and clays subcrop at a 3.39m (ARCA BH04) to 0.92m (ARCA BH03) thickness above the sands and gravel and organic muds. Where the subcrop rests directly on the sands and gravels, and at the upper surface of the inferred palaeosol in ARCA GE BH05, the contact is unconformable, but the contact with the organic mud in ARCA BH04 is conformable. The lower surface of the grey silt/clays varies between 4.34m bgl (+41.04m OD) in ARCA BH04 and 3.36m bgl (+42.00m OD) in ARCA BH03, while the upper contact is between 2.88m bgl (+42.51m OD) in ARCA GE BH05 and 0.95m bgl (+44.43) in ARCA BH04. Nevertheless, there is no representation of depressions seen in the sands and gravels (Section 3.2.1) in the upper contact of the grey silts and clays, except possibly in ARCA GE BH05 (Figure 3).

3.4.2 The grey silts and clays are by no means uniform in their properties. In ARCA BH04 where they are at their thickest, they mostly comprise beds of silt/clay with interspersed granular flint clasts, but strata of clay with sub-angular flint pebbles and granules are interbedded in ARCA BH03, ARCA BH04 and ARCA GE BH05. Iron stains were noted in sand and pebble-sized patches and as wavy, horizontal laminae in the grey silt/clays in all boreholes, while manganese dioxide patches were observed during laboratory description of ARCA GE BH05 and ARCA GE BH06.

3.4.3 The grey silt/clays are the deposits mapped by the BGS as Brickearth (Section 1.3), a category that is thought to have a mixed mode of formation (British Geological Survey 2021b). It is clear from the composite cross section that the Brickearth forms a blanket across the site and is not a second fill of the palaeochannel cut into River terrace deposits 2 (Figure 3). Further, the stratum seems in the most part to have been deposited under gentle depositional energies as witnessed by the survival of a possible palaeosol in the top of the underlying organic muds. Nevertheless, it is likely that the Brickearth formed coevally with Head during the latter stages of its deposition. This conclusion is drawn on the basis that firstly the two strata types interdigitate, and secondly that the matrix of the Head has almost identical properties to the Brickearth. In such a scenario Brickearth would have accreted in the valley bottom and Head on the slopes.

3.4.4 The iron and manganese dioxide stains are features of diagenesis (i.e. are post-depositional) and reflect redox processes (water table movements) operating within the Brickearth. The iron stained laminae are likely highlighting grain size variation

within the stratum and thus while not being primary deposition features of themselves, are highlighting evidence for oscillating depositional energies.

3.5 Head and colluvium

3.5.1 The uppermost stratum, subcropping between the upper contact of the grey silt/clays and the present ground surface is of yellowish brown (10 YR 5/6) matrix-supported gravel of sub-angular flint pebbles and granules in a medium sand to silt matrix. As such the stratum varies between 2.88m (in ARCA GE BH05) and 0.95m (ARCA BH04) in thickness, with the most extensive subcrop being in the central part of the transect and the thinnest at the eastern and western margins.

3.5.2 The matrix-supported gravels are heterogeneous and while the majority of the stratum is poorly sorted, with crude horizontal bedding structures and clasts orientated at various angles, other parts are normally bedded or comprise multiple thin beds with differentiated clast densities. The uppermost 500mm of the stratum has a high proportion of silt/clay, much of which is humic. Iron stains are found throughout both the humic and matrix-supported gravel layers.

3.5.3 The matrix-supported gravels are the Head that is mapped by the BGS and is interpreted by that organisation as having formed in a colluvial depositional environment. Indeed, the poor sorting of the stratum and relative (to the underlying fluvial deposits) angularity of the included gravel particles is indicative of such a genesis. Nevertheless, the varied grain size properties observed in several of the boreholes suggests multiple flow energies as seen in mud- and debris flows (*sensu* Wilkinson 2009). As outlined in Section 3.4.3 during early phases of Head development, colluvial deposition on the slopes of the study area occurred while Brickearth formed in the valley bottom.

3.5.4 The present (Holocene) soil has developed in the top of the Head deposits leading to the humic A horizon described in Section 3.5.2. As the soil formed, worm casting and the formation of humus has led to the development of a predominantly fine-grained capping of the angular matrix-supported gravels.

4. CHRONOSTRATIGRAPHY

Phil Toms, Luminescence Dating Laboratory, University of Gloucestershire

4.1 Summary results of optical dating are presented in Table 3, while as noted above, a full explanation of the methodology, including of estimation of uncertainty, is provided in Appendix 4.

Table 3. Optically stimulated luminescence results of samples from Cutbush Lane East, Shinfield

Lab. Code	Borehole/depth	Total D_r (Gy. ka^{-1})[1]	D_e (Gy)[2]	Age (ka)[3]
GL21068	ARCA GE BH05	1.35±0.12	52.97±3.28	37.1±4.2
GL21069	ARCA GE BH06	0.46±0.05	26.49±1.44	57.0±7.2

[1] Dose rate in Grays per thousand years
[2] Estimated dose in Grays
[3] Age estimate relative to the year of sampling (2021)

5. BIOSTRATIGRAPHY

Rob Batchelor, Quest, University of Reading

5.1 Palynology

5.1.1 The results of the assessment indicate a moderate to high concentration of pollen in four of the samples assessed; only the upper (ARCA GE BH05 4.50m bgl) and lowermost (ARCA GE BH05 5.46m bgl) samples contained a very low concentration of remains (Table 4).

Table 4. Pollen identified in sub-samples from ARCA GE BH05

Latin name	Depth (m bgl) / Common name	4.50	4.63	4.79	4.87	4.95	5.46
Trees							
Pinaceae	pine family						2
Pinus	pine		2			1	
Tilia	lime					1	
Shrubs							
Corylus type	e.g. hazel			1			
Herbs							
Cyperaceae	sedge family		15	7	16	5	1
Poaceae	grass family		10	6	13	6	
Asteraceae	daisy		1	1	3		
Plantago type	plantain		6		2	3	
Lactuceae	dandelion family	1	9		6	2	1
Apiaceae	carrot family		2		2		
Ranunculus type	e.g. buttercup	1	6				
Caryophyllaceae	pink family		1				
Aquatics							
Myriophyllum type	water milfoil		8	2			
Sparganium type	bur-reed		2				
Spores							
Sphagnum	moss				1		
Unknown		1		3	5	2	
Total Land Pollen (grains counted)		3	52	15	42	18	4
Concentration*		1	5	3	5	3	1
Preservation**		2	4	3	3	3	2
Microcharcoal Concentration***		0	1	0	0	0	0
Suitable for further analysis		**NO**	**YES**	**YES**	**YES**	**YES**	**NO**

*Key: *Concentration: 0 = 0 grains; 1 =1-75 grains, 2 = 76-150 grains, 3 =151-225 grains, 4 = 226-300, 5 =300+ grains per slide; **Preservation: 0 = absent; 1 = very poor; 2 = poor; 3 = moderate; 4 = good; 5 = excellent; ***Microcharcoal Concentration: 0 = none, 1= negligible, 2 = occasional, 3 = moderate, 4 = frequent, 5 = abundant*

5.1.2 The samples are characterised by high values of herbaceous and aquatic pollen, dominated by sedges (Cyperaceae), grasses (Poaceae), dandelions (Lactuaceae), plantain (Plantago type), with water milfoil (*Myriophyllum* type), bur-reed (*Sparganium* type), buttercup/water crowsfoot (*Ranunculus* type), carrot family taxa (Apiaceae) and pinks (Caryophyllaceae). Tree and shrub taxa were restricted to a few occurrences of pine (*Pinus*), and individual degraded grains of lime (*Tilia*) and hazel (*Corylus* type). As yet unidentified grains were also noted in most samples.

5.1.3 The results of the assessment are indicative of an open and damp environment, close to still or slowly moving freshwater, and supporting herbaceous and aquatic plants. The samples have the potential to provide further insights into the vegetation and environmental history of the site through increased pollen counts, and identification of unknown taxa..

5.2 Plant macrofossils

5.2.1 The results of the assessment indicate that the samples examined are absent of all macrofossil remains (floral and faunal).

6. ASSESSMENT

6.01 In this section, the results of the field and laboratory investigations are assessed in relation to the aims of the project as set out in Section 1.6.

6.1 Mode of formation of Quaternary strata

6.1.1 The basal Quaternary deposits on the Cutbush Lane East site are fluvial gravels and which as previously noted are attributed to the BGS' Blackwater–Loddon River Terrace 2. The calibre of the gravel particles and their structural arrangement, suggests that they formed as channel bedload during high energy flow, while the thin sand beds are likely to have developed as energies fell, e.g. in the lea of gravel bars or during ebb flow events. Given the relatively small size and shallow gradient of the Blackwater–Loddon catchment, the flow energies required to mobilise the pebbles of the gravel beds were most likely the product of a flashy discharge regime. This latter in lowland England is most usually attributed to a periglacial environment in which high flow events are the product of spring thaw of the permafrost surface (e.g. Bridgland 1994).

6.1.2 The two mean luminescence ages obtained from the fluvial gravels are separated by 20,000 years, but just about overlap at two standard deviation (95% probability) estimates of uncertainty (Figure 4). It is therefore possible that the fluvial gravels accumulated from the end of Marine Isotope Stage (MIS) 4 until mid–late MIS 3, or formed only in MIS 3. Further, the fact that earlier luminescence age mean (GL21069) is at a higher elevation than the later (GL21068), albeit from a different borehole, might indicate that deposition of the gravels was not entirely by vertical accretion, but rather that cut-and-fill events are represented within the stratum. In this latter scenario GL21068 would be an age estimate from the fill of a channel cut into the strata dated by GL21069.

6.1.3 With regards the hypothesis that deposition of the gravels was as a result of periglacial processes, it is of note that MIS 4 was indeed cold and freeze–thaw cycles would be expected in southern England. However, MIS 3 is characterised by rapidly fluctuating climates, comprising temperate episodes (interstadials) as warm as parts of the Holocene as well as cold events (stadials) (Figure 4). Therefore, the high discharge events necessary to deposit gravels during MIS 3 are likely to be the product of surface snow and ice melt and probably during the stadials, but not of permafrost thaw.

6.1.4 As discussed in Section 3.3, the organic muds are also likely to be fluvial strata, but rather deposits that formed under gentle depositional circumstances, such as are found in abandoned channels or another forms of hollow. Indeed, it is quite possible that these fine-grained strata might have been forming on the floodplain at the same time gravel-rich deposits of the type reviewed above accreted in the stream channel elsewhere. Palynological data can be interpreted as support for the inferred alluvial depositional mechanism for the organic muds given the presence of pollen of aquatic and marsh taxa. Although it was not possible to ^{14}C date the organic muds as part of the present investigation (suitable macrofossils not being found - see Section 2.2.4), the palynological assessment identified taxa that are more likely in the warm sub-stages of MIS 3 than the cold environments of MIS 4 or MIS 2. It is also the case that the putative palaeosol in the top of the organic muds in ARCA GE BH05 is more likely to have formed in a relatively warm than cold environment

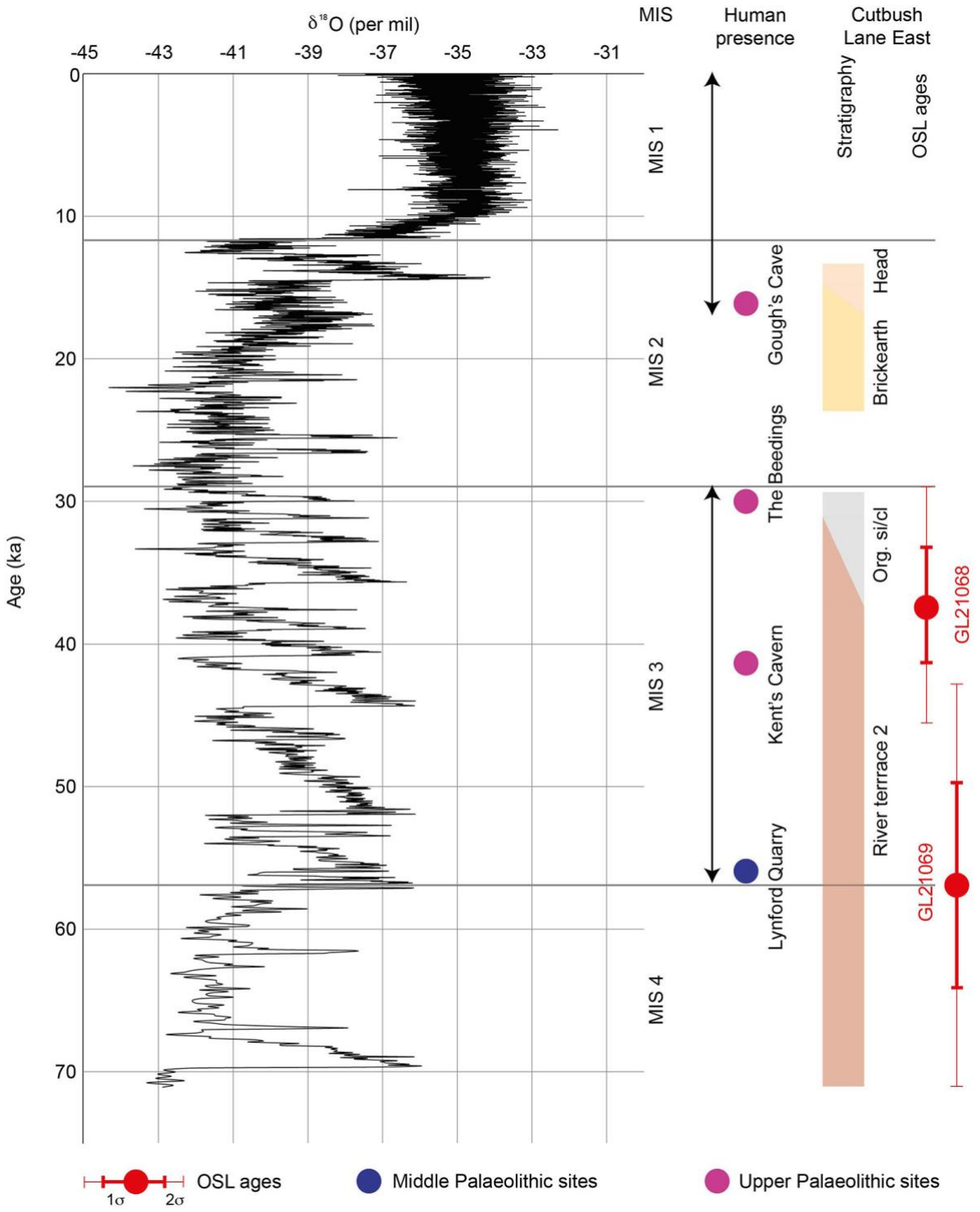

Figure 4. Luminescence dates from the fluvial gravels at Cutbush Lane and hypothetical chronology of the overlying Brickearth and Head plotted against oxygen isotope data from the GRIP ice core and periods of known human occupation in Britain

6.1.5 The Brickearth that caps the fluvial deposits likely formed as a result of a combination of aeolian, colluvial and perhaps fluvial processes (British Geological Survey 2021b). The primary constituent Brickearth is thought to be aeolian and formed of loess blown from glacial outwash settings (Avery et al. 1982). These particles were then reworked and mixed with weathered products of the local bedrock and superficial geology during colluvial and alluvial transport. As set out in Section 3.4.3, the Brickearth sub-crop at

Cutbush Lane East appears as a blanket across the site and does not respect the topography that resulted from prior fluvial deposition. Contacts with the underlying fluvial deposits are also mostly unconformable. In other words, the Brickearth is likely separated in time from the underlying strata while it also probably formed in a different (colder) climate setting than the fluvial deposits. Where dated elsewhere in the Thames valley and in south-eastern England, Brickearth has proven of MIS 2 age (e.g. Gibbard et al. 1987), and the Brickearth strata at Cutbush Lane East tentatively assigned to this period.

6.1.6 The Head deposits that cap the Quaternary sequence at Cutbush Lane East formed as a result of colluvial processes. As has been described in Section 3.4.3, the earliest Head accreted coevally with Brickearth, the combination likely reflecting interdigitating slope deposits (Head) and fluvially reworked loess (Brickearth) in a valley margin setting. The slope instability that gave rise to the Head was probably caused by periglacial processes, i.e. penetration of water into the regolith during the spring–autumn, sub-surface ice formation (and expansion) in the winter months and then melting in the spring to produce debris and mud flows (Ballantyne and Harris 1994). The lower Head deposits at Cutbush Lane East are probably of MIS 2 age, as indeed are most similar Head strata that have been chronometrically dated in southern England (Wilkinson 2009). The upper part of the Head stratum might, however, be colluvium of Holocene age and the product of slope instability as a result of cultivation from the later prehistoric period onwards (Wilkinson 2009).

6.2 Preservation of biological palaeoenvironmental proxies

6.2.1 While an assessment of the macrofossil potential of two samples from the organic mud demonstrated a lack of preservation (further confirming observations made while describing the stratum in the field and laboratory), palynological assessment indicated generally moderate to good preservation. As previously noted (Section 5.1.3), the pollen data indicate that the organic mud formed in a wet environment, which as suggested in Section 6.1.4, was most likely the fill of an abandoned channel or other floodplain hollow. The non-aquatic pollen assemblage is dominated by open ground taxa such as grasses (Poaceae) and members of the buttercup (Ranunculeae) and dandelion (Lactuceae) families, suggesting a meadow-like environment beyond the channel margins. However, there are possible indications in the pollen assemblages for trees and shrubs, namely pine (Pinaceae) in three samples, broad-leafed lime (*Tilia* sp.) and willow (*Corylus* sp.) in one each. Only seven such grains were found (5% of the total pollen identified), while the pine pollen might be from a distant source and the lime and willow grains are weathered. Nevertheless, it is just possible that these arboreal pollen grains might be evidence for the presence of trees in the locality of Cutbush Lane East. If so, the evidence might be an indicator of a cryptic refugium (for thermophilous species) as has been advocated by Stewart and Lister (2001) for parts of continental north western Europe during MIS 3.

6.3 Palaeolithic archaeology and Palaeolithic archaeological potential

6.3.1 It was extremely unlikely that direct evidence of Palaeolithic human activity would be found in borehole auger heads and core samples, and therefore an assessment of archaeological potential has to be made on indirect criteria. These latter are firstly the age of the deposits and whether humans are known to have been in Britain at the relevant time (Figure 4), and secondly the evidence with regards depositional environment provided by the strata revealed in the boreholes. With respect to the latter, *in situ* archaeological evidence is more likely in a floodplain than a channel environment. The text below applies these ideas and the criteria for determining archaeological importance of the draft Historic England guidance for the Palaeolithic

(Hosfield et al. 2020, section 8, 47), to assess the Palaeolithic archaeological potential of the various strata.

6.3.2 The fluvial gravels at the base of the Quaternary sequence at Cutbush Lane East likely formed, as outlined in Section 6.1.1, in a channel setting and during MIS 3 and possibly MIS 4. As Figure 4 indicates, humans were present in Britain during the 57–29 ka time frame of MIS 3 (but not in MIS 4), albeit perhaps not during the stadials. However, the gravels are high energy deposits, which while they might contain reworked artefacts (in common with most other Middle and Late Pleistocene fluvial gravels in the Thames basin [Wymer 1999]), are unlikely to contain *in situ* evidence of human activity. Indeed. there are no indications in the two boreholes that penetrated the entire gravel sequence (ARCA GE BH05 and ARCA GE BH06), for interbedded fine-grained material that might have accreted by a lower energy depositional environment and in which *in situ* archaeological remains might be present. The gravels of River Terrace 2 on the Cutbush Lane East site are therefore assessed as having a low to moderate Palaeolithic archaeological potential.

6.3.3 It has been argued above (Section 6.1.2) that the organic muds subcropping above the fluvial gravels in WA TP1400, ARCA BH02, ARCA GE BH05 and probably WA TP1600 are also of MIS 3 age. They therefore formed during a time frame when humans were at least intermittently present in Britain. Moreover, MIS 3 was an important period of cultural and evolutionary transition. During the 28,000 years of the stage Middle Palaeolithic technologies were succeeded by those of the Upper Palaeolithic, and Neanderthals (*Homo neanderthalensis*) disappeared from the palaeoanthropological record while the range of modern humans (*Homo sapiens*) expanded into western Eurasia (including Britain). The palynology of the organic mud strata suggests that accretion was during warm (interstadial) conditions, i.e. when humans are likely to have been present. Indeed, the organic muds formed under gentle depositional conditions in which *in situ* preservation of archaeological might occur, while there is evidence from ARCA GE BH05 for soil development and therefore a land surface in that location. While humans are unlikely to have undertaken activities that left a trace *within* floodplain pools or abandoned channels, they might have been active on the margins of such features and indeed on the drying surface manifested by the putative palaeosol in ARCA GE BH05. For these reasons and the moderate to good pollen preservation, the organic muds are assessed as having a moderate to high Palaeolithic archaeological potential.

6.3.4 Palaeolithic archaeological sites, some with indications of *in situ* preservation have been found in Brickearth strata, most notably as fills of dolines on interfluve areas of the Chilterns (e.g. Caddington near Luton [Sampson 1978]). In both the Chilterns and the Thames valley, Brickearth is thought to have formed in relatively gentle depositional conditions and that while largely comprised of re-worked sediment, stratification is preserved (White 1997). However, the Chiltern brickearths that contain Palaeolithic archaeological remains are attributed to the Middle Pleistocene (White 1997), while those at Cutbush Lane East must be MIS 3 later given the OSL ages on the basal fluvial gravels. Indeed, they are argued to be of MIS 2 age in Section 6.1.5, in which case they probably formed during a time frame when humans were not present in Britain (Figure 4). For these reasons the Brickearth at Cutbush Lane East is assessed as having a low Palaeolithic archaeological potential.

6.3.5 The Head deposits at Cutbush Lane East formed as a result of erosion of the western slopes of the Loddon valley and subsequent transport of the resulting sediment downslope. The deposits are of mixed calibre and are poorly sorted, while there are no indications in the six ARCA boreholes for stabilisation episodes (as are sometimes noted in late MIS 2 head deposits on the Chalk downland of Kent and Sussex [e.g.

Preece and Bridgland 1998]). It is therefore unlikely that *in situ* Palaeolithic artefacts will be found in the Head deposits of Cutbush Lane East. Further, as discussed in Section 6.1.6, the Head strata are likely to be of MIS 2 age, and therefore forming in a period when humans were largely absent in Britain. The Head at Cutbush Lane East is therefore assessed as having a low Palaeolithic archaeological potential.

7. CONCLUSIONS

7.1 The geoarchaeological borehole study of a 40m-wide strip of land immediately west of Cutbush Lane East, Shinfield demonstrates that a 4–5m thick sequence of Quaternary deposits overlie London Clay Formation (Eocene) bedrock. The Quaternary strata are largely of Pleistocene age and comprise 1.1–1.5m of fluvial gravel dating from MIS 3 (and possibly MIS 4), overlain by 0.47–0.17m of organic silt/clay, also probably dating from MIS 3. These two deposits likely formed while humans were present in southern England, but *in situ* preservation is more likely to be associated with the latter than the former. Overlying the fluvial sequence are 3.39–0.92m of Brickearth and 2.88–0.95m of Head, these forming as a result of aeolian, colluvial and possibly alluvial processes, and most likely during MIS 2. Humans are only thought to have inhabited Britain during the final parts of MIS 2, and therefore it is considered that these strata are unlikely to contain in situ Palaeolithic archaeological remains.

7.2 The strata assessed as being of moderate–high Palaeolithic archaeological potential lie at 4.3–5.0m bgl and in a 32m+ wide swathe stretching from east of ARCA BH01 to west of ARCA BH03. These deposits are (a) below the current water table (measured at 3–4m bgl during fieldwork), (b) at a depth that would make trenching/test pitting an extremely challenging undertaking, and (c) only likely to be encountered during construction should piles be driven at the relevant location. It is therefore recommended that any impact on the moderate–high potential deposits is mitigated by further study of the currently available samples and publication of the data in a peer reviewed journal in open access form. Publication is in any case highly desirable given that (i) MIS3 fluvial deposits are rare in southern Britain (early MIS3 strata at Lynford Quarry, Norfolk are the best known example [Boismier et al. 2012]), (ii) as noted in Section 6.3.3, MIS 3 is of great importance period from a cultural and evolutionary perspective, (iii) the OSL chronology from Cutbush Lane East is the first from Pleistocene deposits of the Blackwater–Loddon and (iv) the tentative evidence of the palynological assessment for trees. If confirmed by more detailed palynological study, these latter would be the first such evidence for trees in Britain in MIS3.

8. ACKNOWLEDGMENTS

8.1 ARCA would like to thank the following for their help prior to and during the fieldwork reported here: Tony Brown and Ray Kennedy (Cotswold Archaeology), Wayne Fitton, Nick and Jamie (Geotechnical Engineering Ltd.).

8.2 Fieldwork at Cutbush Lane East was carried out by Prof Keith Wilkinson and William Reid. Laboratory description and sub-sampling of cores was undertaken by Keith Wilkinson.

9 REFERENCES

Avery, L., Bullock, P., Catt, J.A., Rayner, J.H. and Weir, A.H. (1982) Composition and origin of some brickearths on the Chiltern Hills, England. *Catena* 9,153-174.

Ballantyne, C.K. and Harris C. (1994) *The Periglaciation of Great Britain*. Cambridge University Press.

Boismier, W.A., Gamble, C. and Coward, F. (Eds.) (2012) *Neanderthals among mammoths: excavations at Lynford Quarry, Norfolk UK*, English Heritage Monograph, London,

Bridgland, D.R. (1994) *Quaternary of the Thames*. Chapman and Hall, London.

British Geological Survey (2017a) iGeology. http://www.bgs.ac.uk/igeology/ (accessed 1 September 2021)

British Geological Survey (2021a) iGeology. http://www.bgs.ac.uk/igeology/ (accessed 1 September 2021)

British Geological Survey (2021b) The BGS Lexicon of named rock units. http://www.bgs.ac.uk/lexicon/home.cfm (accessed 2 September 2021).

Campbell, G., Moffett, L. and Straker, V. (2011) Environmental archaeology: A guide to the theory and practice of methods, from sampling and recovery to post-excavation. Second edition. https://historicengland.org.uk/images-books/publications/environmental-archaeology-2nd/. (accessed 2 September 2021)

CIfA (2014) Standard and guidance for archaeological field evaluation. https://www.archaeologists.net/sites/default/files/CIfAS&GFinds_1.pdf (accessed 2 September 2021).

Dawkins, T., Legg, E. and Shaw, A. (2021) Shinfield Studios Creative Media Hub, Shinfield, Berkshire: archaeological evaluation and geoarchaeological test pitting. Unpublished report 242982.03, Wessex Archaeology, Salisbury.

Historic England (2015) Geoarchaeology: using Earth Sciences to understand the archaeological record. Second Edition. https://historicengland.org.uk/images-books/publications/geoarchaeology-earth-sciences-to-understand-archaeological-record/. (Accessed 2 September 2021).

Gibbard, P.L., Wintle, A.G. and Catt, J.A. (1987) Age and origin of clayey silt, 'brickearth' in west London, England. *Journal of Quaternary Science* 2, 3-9.

Hosfield, R., Green, C., Fluck, H. and Batchelor, C.R. (2020) Curating the Palaeolithic: guidance (consultation draft). https://historicengland.org.uk/content/docs/guidance/curating-the-palaeolithic-consultation-draft/ (accessed 1 September 2021).

Jones, A.P., Tucker, M.E. and Hart, J.K. (1999) Guidelines and recommendations. In Jones, A.P., Tucker, M.E. and Hart, J.K. (Eds.) *The description and analysis of Quaternary stratigraphic field sections*. Quaternary Research Association technical guide **7**, London, 27-76.

Moore, P.D., Webb, J.A. and Collinson, M.E. (1991) *Pollen Analysis*. Second Edition. Blackwell, Oxford.

Munsell Color (2000) *Munsell soil color charts*. Munsell Color, New Windsor (NY).

Preece, R.C. and Bridgland, D.R. (1998) *Late Quaternary environmental change in North-west Europe: excavations at Holywell Coombe, South-east England*. Chapman and Hall, London.

Reille, M. (1992) *Pollen et Spores d'Europe et d'Afrique du Nord*. Laboratoire de Botanique Historique et Palynologie, Marseille.

Rockware (2017) RockWorks v17. http://www.rockware.com (Accessed 7 February 2017).

Stace, C. (2005) *New Flora of the British Isles*. Cambridge University Press, Cambridge.

Sampson, C.G. (Ed.) (1978) *Paleoecology and Archaeology of an Acheulian Site at Caddington, England*. Department of Anthropology, Southern Methodist University, Dallas (TX).

Stewart, J.R. and Lister, A.M. (2001) Cryptic northern refugia and the origins of the modern biota. *Trends in Ecology & Evolution* 16, 608–613.

Tucker, M.E. (2011) *Sedimentary rocks in the field*. Fourth Edition. Wiley, Chichester.

Wenban-Smith, F.F. (2014) The Lower/Middle Palaeolithic research agenda. In Hey, G. and Hind, G. (Eds). *Solent-Thames Research Framework for the Historic Environment Resource Assessments and Research Agendas.* Oxford Wessex Archaeology, Oxford, 53–59.

Wenban-Smith, F.F., Hardaker, T., Hosfield, R.T., Loader, R., Silva, B., Wilkinson, K.N., Bridgland, D.R., Cramp, K. and Allen, M.J. (2014) The Lower/Middle Palaeolithic: research agenda. In Hey, G. and Hind. J. (Eds.) *Solent-Thames Research Framework for the Historic Environment: resource assessments and research agendas*. Oxford Wessex Monograph 6, Oxford, 53–59

White, M. (1997) The earlier Palaeolithic occupation of the Chilterns (southern England): re-assessing the sites of Worthington G. Smith. *Antiquity* 71, 912-931.

Wilkinson, K.N. (2009) Regional review of geoarchaeology in the Southern Region: colluvium. Historic England Research Department Report 3/2009. Historic England, Portsmouth. Available at: https://research.historicengland.org.uk/Report.aspx?i=14719&ru=%2FResults.aspx%3Fp%3D402.

Wilkinson, K.N. (2021) Land west of Cutbush Lane, Shinfield, Reading: geoarchaeological borehole study. Written scheme of investigation and risk assessment method statement. Unpublished document, ARCA, University of Winchester.

Wilkinson, K.N., Watson, N., Bethell, P. and Toms, P. (2018) Modelling Pleistocene deposits and the Palaeolithic archaeological potential of a site at Pan Lane, 39 Newport, Isle of Wight. In Carey, C., Howard, A.J., Knight, D., Corcoran, J. and Heathcote, J. (Eds.) *Deposit modelling and archaeology*, University of Brighton, Brighton, 39-50.

Wymer, J.J. (1999) *The Lower Palaeolithic occupation of Britain*. Wessex Archaeology and English Heritage, Salisbury.

APPENDIX 1: BOREHOLE LOCATIONS

Borehole	Easting	Northing	Elevation[a]
ARCA BH01	474167.70	169203.60	+45.540
ARCA BH02	474194.50	169233.30	+45.267
ARCA BH03	474221.20	169263.00	+45.355
ARCA BH04	474248.00	169292.80	+45.377
ARCA GE BH05	474185.90	169220.60	+45.389
ARCA GE BH06	474227.90	169270.10	+45.360

[a] Ordnance Datum elevation of borehole collar.

APPENDIX 2: BOREHOLE LITHOSTRATIGRAPHY

Borehole	Top	Base	Lithology	Comments
ARCA BH01	0.00	0.50	Soil	10 YR 4/4 Dark yellowish brown humic silt/clay with occasional granular- and pebble-sized sub-angular flint. Iron stained mottles throughout. Moderately sorted. Sharp boundary to (Topsoil):
ARCA BH01	0.50	1.95	Matrix-supported gravel	7.5 YR 4/4 Brown matrix-supported gravel of sub-angular and sub-rounded flint pebbles and granules in a silt/clay to granular matrix. Structured as thin beds of different densities of clasts. Poorly sorted. Sharp boundary to (Head):
ARCA BH01	1.95	2.00	Silt/clay	7.5 YR 5/6 Strong brown silt/clay with occasional fine pebble-sized sub-angular flint clasts. Moderately sorted. End of core (Brickearth):
ARCA BH01	2.00	4.50	Silt/clay	10 YR 5/2 Greyish brown silt/clay, reverse bedded and becoming clay 2-3m. Frequent iron staining as general cover 7.5 YR 5/4 Brown at 2-3m and as wavy parallel, vertical and sub-horizontal coarse laminae below. Frequent coarse sand MnO_2 stains throughout. Rare sub-angular flint-sized pebbles. Well sorted. Sharp boundary to (Brickearth):
ARCA BH01	4.50	4.70	Sand	2.5 Y 5/2 Greyish brown medium sand oxidising to 7.5 YR 4/6 Strong brown. Reverse bedded, i.e. coarsening upwards to medium sand with moderate granular-sized sub-angular flint. Iron stained as thin, wavy, sub-horizontal beds. Sharp boundary to (Pleistocene terrace):
ARCA BH01	4.70	4.85	Clast-supported gravel	Clast-supported gravel of sub-rounded and sub-angular flint pebbles and granules in a medium sand-silt matrix. Poorly sorted. Sharp boundary to (Pleistocene terrace):
ARCA BH01	4.85	5.00	Matrix-supported gravel	10 YR 5/6 Yellowish brown matrix-supported gravel of sub-angular and sub-rounded granular flint clasts in a medium-coarse sand matrix. Crude verse bedded, i.e. matrix more frequent at base and clasts become larger up core. Poorly sorted. End of core (Pleistocene terrace).
ARCA BH02	0.00	0.40	Soil	10 YR 4/2 Dark greyish brown humic silt/clay and fine sand with occasional pebble-sized sub-angular brick clasts. Moderately sorted. Diffuse boundary to (Topsoil):
ARCA BH02	0.40	0.44	Diamict	10 YR 4/3 Brown diamict/matrix-supported gravel of sub-angular and sub-rounded concrete pebbles, brick pebbles in a silt/clay matrix. Poorly sorted. Sharp boundary to (Made ground):

Borehole	Top	Base	Lithology	Comments
ARCA BH02	0.44	1.50	Matrix-supported gravel	7.5 YR 4/6 Strong brown matrix-supported gravel of sub-angular flint pebbles, granules and fine cobbles in a medium/coarse sand-silt/clay matrix. Poorly sorted. Sharp boundary to (Head):
ARCA BH02	1.50	1.66	Clay	7.5 YR 5/6 Strong brown silty clay with moderate granular and fine-pebble sized sub-angular flint. Poorly sorted. Sharp boundary to (Brickearth/Head):
ARCA BH02	1.66	2.21	Matrix-supported gravel	7.5 YR 5/6 Strong brown matrix-supported gravel of sub-angular and sub-rounded flint pebbles in a silt/clay matrix. Poorly sorted. Sharp boundary to (Head):
ARCA BH02	2.21	3.34	Clay	7.5 YR 5/6 Strong brown silty clay with occasional sub-rounded and sub-angular fine pebble-sized flint, decreasing downwards. Compact. Well sorted. Diffuse boundary to (Brickearth):
ARCA BH02	3.34	4.20	Silt/clay	10 YR 5/3 Brown silt/clay with moderate iron stains. Well sorted. Diffuse boundary to (Brickearth):
ARCA BH02	4.20	4.33	Silt/clay	10 YR 4/2 Dark greyish brown silt/clay with moderatefine fibrous plant material. Well sorted. Diffuse boundary to (Alluvium):
ARCA BH02	4.33	4.60	Organic silt/clay	2.5 Y 3/1 Very dark grey silt/clay with frequent fibrous plant remains. Well sorted. Sharp boundary to (Alluvium):
ARCA BH02	4.60	4.65	Silt/clay	10 YR 5/6 Yellowish brown silt/clay. Well sorted. Sharp boundary to (Alluvium):
ARCA BH02	4.65	4.70	Clast-supported gravel	Clast- and matrix-supported gravel of sub-rounded and sub-angular flint pebbles in a silt/clay matrix. Poorly sorted. Hole abandoned as gravel is impenetrable (Pleistocene terrace).
ARCA BH03	0.00	0.32	Soil	10 YR 4/3 Brown humic silt/clay and fine sand with occasional granular and fine pebble-sized sub-angular and sub-rounded flint clasts. Moderately sorted. Sharp boundary to (Topsoil):
ARCA BH03	0.32	1.10	Matrix-supported gravel	7.5 YR 5/6 Strong brown clast- and matrix-supported gravel of sub-angular and sub-rounded flint pebbles and granules in a silt/clay matrix. Poorly sorted. Sharp boundary to (Head?):

Borehole	Top	Base	Lithology	Comments
ARCA BH03	1.10	1.32	Sand	7.5 YR 5/6 Strong brown medium sand with moderate sub-angular and sub-rounded flint pebbles and granules, decreasing upwardss (normally bedded). Poorly sorted. Sharp boundary to (Head?):
ARCA BH03	1.32	1.42	Clay	10 YR 5/6 Yellowish brown silt/clay. Compact. Iron stained. Well sorted. Sharp boundary to (Brickearth/Head):
ARCA BH03	1.42	1.49	Matrix-supported gravel	10 YR 4/6 Strong brown matrix-supported gravel of sub-angular fine pebble and granular-sized flint clasts in a silt/clay matrix. Poorly sorted. Sharp boundary to (Head):
ARCA BH03	1.49	1.64	Silt/clay	10 YR 5/6 Strong brown silt/clay with rare sub-angular flint pebbles. Iron stained. Moderately sorted. Sharp boundary to (Brickearth/Head):
ARCA BH03	1.64	2.44	Matrix-supported gravel	7.5 YR 4/6 Strong brown matrix-supported gravel of sub-angular and sub-rounded flint pebbles and granules in a silt/clay matrix. Poorly sorted. Sharp boundary to (Head):
ARCA BH03	2.44	3.36	Silt/clay	2.5 Y 6/3 Light yellowish brown, changing upwards to 10 YR 5/6 Strong brown (oxidation) silt/clay. Iron stained as horizontal, discontinuous wavy and straight lamina. Normally bedded, i.e. slight fine sand content at base, but disappearing upwards. Well sorted. Diffuse boundary to (Brickearth):
ARCA BH03	3.36	3.52	Sand	7.5 YR 5/8 Strong brown fine-medium sand. Well sorted. Iron stained. Diffuse boundary to (?Brickearth/Pleistocene terrace):
ARCA BH03	3.52	3.78	Matrix-supported gravel	7.5 YR 4/6 Strong brown matrix-supported gravel of sub-rounded flint pebbles in a granular and coarse sand matrix. Poorly sorted. Sharp boundary to (Pleistocene terrace):
ARCA BH03	3.78	3.90	Sand	10 YR 4/6 Strong brown medium sand with rare granular-sized sub-angular flint. Well sorted (Pleistocene terrace).
ARCA BH03	3.90	4.00	No recover	Void. Hole abandoned at 4.00m as it had proved very difficult to drill through the compact sands and gravels of 3.52-4.00m.
ARCA BH04	0.00	0.28	Soil	10 YR 4/3 Brown humic silt/clay and fine sand with moderate sub-rounded and sub-angular flint pebbles. Moderately sorted. Sharp boundary to (Topsoil):

Borehole	Top	Base	Lithology	Comments
ARCA BH04	0.28	0.50	Silt/clay	10 YR 5/4 Yellowish brown silt/clay and fine sand with fine vertical iron-stained lines (root channels). Moderately sorted. Diffuse boundary to (Colluvium with pedogenesis):
ARCA BH04	0.50	0.77	Silt/clay	10 YR 6/6 Brownish yellow calcareous silt/clay with frequent iron stains - in patches around aggregates and as horizontal lines. Sharp boundary to (Colluvium with pedogenesis):
ARCA BH04	0.77	0.95	Matrix-supported gravel	10 YR 5/4 Yellowish brown matrix-supported gravel of sub-angular and sub-rounded flint pebbles is a silt/clay and fine sand matrix. Frequent iron stains around clasts. Poorly sorted. Sharp boundary to (Colluvium/Head):
ARCA BH04	0.95	1.60	Silt/clay	7.5 YR 5/6 Strong brown silt/clay with occasional granular-size sub-angular flint clasts, increasing upwards. Iron stained throughout. Moderately sorted. Diffuse boundary to (Brickearth):
ARCA BH04	1.60	4.00	Silt/clay	7.5 YR 5/6 Strong brown silt/clay. Iron stained throughout. Rare sub-angular flint granules. Granular to coarse sand sized iron stains at 2.00-2.50m, and concentrations of pebble-sized flints clasts at 3.50-3.60 and 3.89-3.91m. Moderately sorted. (Brickearth):
ARCA BH04	4.00	4.34	Silt/clay	7.5 YR 5/4 Brown silt/clay with rare granular-sized flint clasts. Iron-stained as coarse sand-sized patches and discontinuous coarse horizontal laminae/fine layers at base. Well sorted. Sharp boundary to (Brickearth):
ARCA BH04	4.34	4.44	Sand	10 YR 5/6 Yellowish brown finely bedded medium sand with rare coarse sand-sized flint clasts and single coarse horizontal lamina of 7.5 YR 5/4 Brown silt. Sand sets differentiated on the base of gravel clast content. Well-moderately sorted. Sharp boundary to (Pleistocene terrace):
ARCA BH04	4.44	4.46	Silt/clay	7.5 YR 5/3 Brown thickly bedded silt, iron stained at surface as a thin horizontal bed. Well sorted. Sharp boundary to (Pleistocene terrace):
ARCA BH04	4.46	4.83	Sand	10 YR 5/4 Yellowish brown medium sand with moderate to rare sub-rounded flint granules. Forming thin-medium bedded set differentiated by clast content and iron staining. Well sorted. Sharp boundary to (Pleistocene terrace):
ARCA BH04	4.83	5.00	Clast-supported gravel	2.5 Y 5/4 Light olive brown matrix and clast-supported gravel of sub-angular and sub-rounded flint pebbles and granules in a medium sand matrix. Single, discontinuous coarse lamina of 7.5 YR 5/3 Brown silt at 4.86m. End of core (Pleistocene terrace).

Borehole	Top	Base	Lithology	Comments
ARCA GE BH05	0.00	1.20	Inspection pit	Hand dug inspection pit - not logged
ARCA GE BH05	1.20	1.89	Matrix-supported gravel	7.5 YR 4/3 Brown matrix-supported gravel of sub-angular and sub-rounded flint pebbles and granules in a silt to medium sand matrix. Clasts orientated at various angles. Poorly sorted. Sharp boundary to (Head):
ARCA GE BH05	1.89	2.27	Clay	10 YR 5/6 Yellowish brown silty clay. Iron stained throughout. Compact. Homogeneous. Well sorted. Diffuse boundary to (Brickearth/Head):
ARCA GE BH05	2.27	2.42	Silt/clay with gravel	7.5 YR 5/4 Brown silty clay with frequent sub-angular fine pebble and granular-sized flint clasts. Poorly sorted. Iron-stained around clasts. Diffuse boundary to (Brickearth/Head):
ARCA GE BH05	2.42	2.70	Clay	5 Y 5/1 Grey oxidising to 10 YR 5/6 Strong brown silt/clay with rare sub-angular flint granules. Iron stained throughout and moderate granular-size MnO_2 stains. Moderately sorted. End of core (Brickearth).
ARCA GE BH05	2.70	2.88	Matrix-supported gravel	10 YR 4/6 Dark yellowish brown matrix-supported gravel of sub-angular and sub-rounded flint pebbles and granules in a silt-clay matrix. Distinct matrix-rich fine layer at 2.78-2.82m. Clasts variably orientated. Poorly sorted. Sharp boundary to (Brickearth/Head):
ARCA GE BH05	2.88	4.20	Silt/clay	2.5 Y 6/1 Grey oxidising to 7.5 YR 4/6 Strong brown silt/clay. Iron stains present as wavy, sub-horizontal, discontinuous coarse laminae to thin layers. MnO_2 stains as coarse sand-sized patches scattered throughout. Rare sub-angular flint pebbles and granules. Moderately sorted. End of core (Brickearth).
ARCA GE BH05	4.20	4.37	No recover	Void
ARCA GE BH05	4.37	4.57	Silt/clay	2.5 Y 6/1 Grey oxidising to 7.5 YR 4/6 Strong brown silt/clay. Iron stains present as wavy, sub-horizontal, discontinuous coarse laminae to thin layers. MnO2 stains as coarse sand-sized patches scattered throughout. Rare sub-angular flint pebbles and granules. Coarse, straight, horizontal lamina of granular and coarse sand-sized flint clasts at interface with underlying unit. Moderately sorted. Sharp boundary to (Brickearth):

Borehole	Top	Base	Lithology	Comments
ARCA GE BH05	4.57	4.61	Ripened silt/clay	2.5 Y 4/2 Dark greyish brown with 'ripened' lower part of 7.5 YR 4/2 Brown silt/clay. Well sorted. Ripening is a thin, continuous, horizontal layer at the base. Diffuse boundary to (Palaeosol in alluvium):
ARCA GE BH05	4.61	5.03	Organic silt/clay	5 Y 4/1 Dark grey organic silt/clay containing granular sized patches of completely decomposed organics increasing downwards to dominate the layer. Rare sub-angular pebble-sized flint clasts. Moderately sorted. Sharp boundary to (Alluvium):
ARCA GE BH05	5.03	5.44	Clast-supported gravel	Clast-supported gravel of 50-100mm-thick sets of sub-rounded and occasional sub-angular flint pebbles and granules in medium to coarse sand matrix. Sets differentiated on the basis of gravel grain size and matrix content. Moderately sorted within sets. Sharp boundary to (Pleistocene terrace):
ARCA GE BH05	5.44	5.55	Fine sand/silt	10 YR 5/3 Brown fine sand/silt with occasional sub-angular flint granules. Well sorted. Sharp boundary to (Pleistocene terrace):
ARCA GE BH05	5.55	5.70	Clast-supported gravel	Clast-supported gravel of sub-rounded flint pebbles and granules in a coarse sand matrix. Sands partially washed out during drilling and stratum has collapsed. End of core (Pleistocene terrace).
ARCA GE BH05	5.70	6.08	No recover	Void
ARCA GE BH05	6.08	6.15	Clast-supported gravel	Clast-supported gravel of sub-rounded flint pebbles and granules in a coarse sand to silt matrix. Poorly sorted. Sharp boundary to (Pleistocene terrace):
ARCA GE BH05	6.15	7.00	Mudstone	5 Y 5/1 Grey compact silt/clay. Homogeneous. Well sorted. End of core (London Clay).
ARCA GE BH06	0.00	1.20	Inspection pit	Hand dug inspection pit - not logged
ARCA GE BH06	1.20	1.83	Clay	7.5 YR 4/6 Strong brown silty clay with rare sub-angular and sub-rounded flint pebbles. Iron stained throughout. Homogeneous. Moderately sorted. Diffuse boundary to (Brickearth/Head):

Borehole	Top	Base	Lithology	Comments
ARCA GE BH06	1.83	2.19	Matrix-supported gravel	7.5 YR 5/4 Brown matrix-supported gravel of sub-angular and sub-rounded flint pebbles and granules in a silty clay matrix. Normally bedded, ie gravel density and calibre decreases upwards. Poorly sorted. Sharp boundary to (Head/Brickearth):
ARCA GE BH06	2.19	3.62	Silt/clay	10 YR 5/2 Greyish brown, oxidising to 7.5 YR 5/4 Brown silt/clay with rare sub-angular flint pebbles. Iron stained throughout, as crude, wavy, parallel, discontinuous, sub-horizontal coarse laminae to fine layers and surface coating. Coarse sand-sized MnO_2 patches throughout. Moderately sorted. Sharp boundary to (Brickearth):
ARCA GE BH06	3.62	4.08	Matrix-supported gravel	10 YR 4/6 Dark yellowish brown matrix-supported gravel of sub-angular and sub-rounded flint pebbles and granules in a medium sand matrix. Formed of sets of 50-150mm thickness differentiated by density and calibre of gravels. Below 3.87m gravels are predominantly granules. Moderately to poorly sorted within sets. Sharp boundary to (Pleistocene terrace):
ARCA GE BH06	4.08	4.16	Sand	2.5 Y 5/3 Light olive brown medium sand with occasional granular and coarse sand-sized flint clasts. Moderately sorted. Sharp boundary to (Pleistocene terrace):
ARCA GE BH06	4.16	4.38	Matrix-supported gravel	7.5 YR 5/6 Strong brown matrix-supported gravel of sub-rounded and sub-angular flint pebbles and granules in a medium sand matrix. Poorly sorted. Diffuse boundary to (Pleistocene terrace).
ARCA GE BH06	4.38	4.70	Clast-supported gravel	Clast-supported gravel of sub-rounded flint pebbles and granules in a medium sand matrix. Formed of 20--30mm thick sets differentiated by gravel density and calibre. Moderately sorted. Diffuse boundary to (Pleistocene terrace):
ARCA GE BH06	4.70	5.24	Matrix-supported gravel	10 YR 5/2 Greyish brown matrix-supported gravel of sub-angular and sub-rounded flint pebbles and granules in a medium-fine sand matrix. Gravel density varies with depth, but no sets and homogeneous. Poorly sorted. Sharp boundary to (Pleistocene terrace):
ARCA GE BH06	5.24	5.54	Clast-supported gravel	Clast-supported gravel of sub-angular and sub-rounded flint pebbles and granules in rare coarse sand matrix. Normally bedded, grading from pebble- to fine pebble-granular gravel. Moderately sorted. Sharp boundary to (Pleistocene terrace):

Borehole	Top	Base	Lithology	Comments
ARCA GE BH06	5.54	5.67	Matrix-supported gravel	7.5 YR 4/4 Brown matrix-supported gravel of sub-angular flint granules and fine pebbles in a medium-fine sand matrix. Poorly sorted. Sharp boundary to (Pleistocene terrace):
ARCA GE BH06	5.67	5.72	Mudstone	7.5 YR 4/4 Brown compact silt/clay. Well sorted. Diffuse boundary to (London Clay):
ARCA GE BH06	5.72	5.92	Mudstone	5 Y 4/1 Dark grey compact silt/clay. Well sorted. End of core (London Clay).

APPENDIX 3: BOREHOLE CORE PHOTOGRAPHS

A3.1: ARCA BH01

Top[b]		Base[b]
0.00		0.50
0.50		1.00
1.00		2.00
4.00 3.00 2.00		5.00 4.00 3.00

[b] m bgl

A3.2: ARCA BH02

Top[b]		Base[b]
0.00		1.00
1.00		2.00
2.00		3.00
3.00		4.00
4.00		4.70

[b] m bgl

A3.3: ARCA BH03

Top[b]		Base[b]
0.00		0.50
0.50		1.00
1.00		2.00
2.00		3.00
3.00		4.00

[b] m bgl

A3.4: ARCA BH04

Top[b]		Base[b]
0.00		0.50
0.50		1.00
1.00		2.00
2.00		3.00
3.00		4.00
4.00		5.00

[b] m bgl

A3.5: ARCA GE BH05

Top[b]		Base[b]
1.20 2.70		2.70 4.20
4.20 5.70		5.70 7.00

[b] m bgl

A3.6: ARCA GE BH06

Top[b]		Base[b]
1.20 1.50	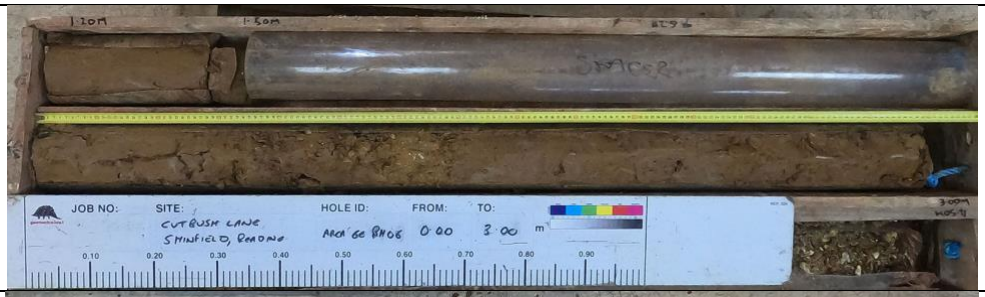	1.50 3.00
3.00 4.50		4.50 6.00

[b] m bgl

APPENDIX 4: OPTICAL DATING REPORT

The original report on the OSL dating of the samples from Cutbush Lane East is appended overleaf.

University of Gloucestershire

Luminescence dating laboratory

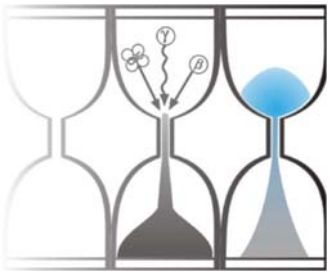

Optical dating of sediments: Cutbush Lane boreholes, UK

to

Prof. Keith Wilkinson

ARCA

Analysis & Reporting, Prof. P.S. Toms
Sample Preparation & Measurement, Dr J.C. Wood
03 February 2022

Contents

Scope of Report

This is a standard report of the Luminescence dating laboratory, University of Gloucestershire. In large part, the document summarises the processes, diagnostics and data drawn upon to deliver Table 1. A conclusion on the analytical validity of each sample's optical age estimate is expressed in Table 2; where there are caveats, the reader is directed to the relevant section of the report that explains the issue further in general terms.

Copyright Notice

Field Code	Lab Code	Overburden (m)	Grain size (μm)	Moisture content (%)	Ge γ-spectrometry (*ex situ*)			β D_r (Gy.ka^{-1})	γ D_r (Gy.ka^{-1})	Cosmic D_r (Gy.ka^{-1})	Preheat (°C for 10s)	Low Dose Repeat Ratio	High Dose Repeat Ratio	Post-IR OSL Ratio
					K (%)	Th (ppm)	U (ppm)							
OSL 1	GL21068	5.48	180-250	16 ± 4	1.13 ± 0.08	4.01 ± 0.38	0.75 ± 0.09	0.81 ± 0.10	0.46 ± 0.08	0.09 ± 0.01	220	1.02 ± 0.04	1.04 ± 0.04	0.99 ± 0.04
OSL 2	GL21069	4.10	180-250	16 ± 4	0.31 ± 0.05	1.22 ± 0.31	0.21 ± 0.08	0.23 ± 0.05	0.13 ± 0.05	0.11 ± 0.01	200	0.96 ± 0.04	1.02 ± 0.04	0.96 ± 0.04

Field Code	Lab Code	Total D_r (Gy.ka^{-1})	D_e (Gy)	Age (ka)
OSL 1	GL21068	1.35 ± 0.12	52.97 ± 3.28	37.1 ± 4.2 (3.7)
OSL 2	GL21069	0.46 ± 0.05	26.49 ± 1.44	57.0 ± 7.2 (6.7)

Table 1 D_r, D_e and Age data of submitted samples located at c. 51°N, 1°W, 46m. Age estimates expressed relative to year of sampling. Uncertainties in age are quoted at 1σ confidence, are based on analytical errors and reflect combined systematic and experimental variability and (in parenthesis) experimental variability alone (see 6.0). **Blue** indicates samples with accepted age estimates, **red**, age estimates with caveats (see Table 2).

Generic considerations	Field Code	Lab Code	Sample specific considerations
Absence of *in situ* γ spectrometry data (see section 4.0)	OSL 1	GL21068	None
	OSL 2	GL21069	None

Table 2 Analytical validity of sample suite age estimates and caveats for consideration

1.0 Mechanisms and principles

Upon exposure to ionising radiation, electrons within the crystal lattice of insulating minerals are displaced from their atomic orbits. Whilst this dislocation is momentary for most electrons, a portion of charge is redistributed to meta-stable sites (traps) within the crystal lattice. In the absence of significant optical and thermal stimuli, this charge can be stored for extensive periods. The quantity of charge relocation and storage relates to the magnitude and period of irradiation. When the lattice is optically or thermally stimulated, charge is evicted from traps and may return to a vacant orbit position (hole). Upon recombination with a hole, an electron's energy can be dissipated in the form of light generating crystal luminescence providing a measure of dose absorption.

Herein, quartz is segregated for dating. The utility of this minerogenic dosimeter lies in the stability of its datable signal over the mid to late Quaternary period, predicted through isothermal decay studies (e.g. Smith *et al*., 1990; retention lifetime 630 Ma at 20°C) and evidenced by optical age estimates concordant with independent chronological controls (e.g. Murray and Olley, 2002). This stability is in contrast to the anomalous fading of comparable signals commonly observed for other ubiquitous sedimentary minerals such as feldspar and zircon (Wintle, 1973; Templer, 1985; Spooner, 1993)

Optical age estimates of sedimentation (Huntley *et al*., 1985) are premised upon reduction of the minerogenic time dependent signal (Optically Stimulated Luminescence, OSL) to zero through exposure to sunlight and, once buried, signal reformulation by absorption of litho- and cosmogenic radiation. The signal accumulated post burial acts as a dosimeter recording total dose absorption, converting to a chronometer by estimating the rate of dose absorption quantified through the assay of radioactivity in the surrounding lithology and streaming from the cosmos.

$$\text{Age} = \frac{\text{Mean Equivalent Dose } (D_e, \text{Gy})}{\text{Mean Dose Rate } (D_r, \text{Gy.ka}^{-1})}$$

Aitken (1998) and Bøtter-Jensen *et al*. (2003) offer a detailed review of optical dating.

2.0 Sample Preparation

Two sediment samples were collected within opaque tubing and submitted for Optical dating. To preclude optical erosion of the datable signal prior to measurement, all samples were opened and prepared under controlled laboratory illumination provided by Encapsulite RB-10 (red) filters. To isolate that material potentially exposed to daylight during sampling, sediment located within 10 mm of each tube-end was removed.

The remaining sample was dried and then sieved. The fine sand fraction was segregated and subjected to acid and alkaline digestion (10% HCl, 15% H_2O_2) to attain removal of carbonate and organic components respectively. A further acid digestion in HF (40%, 60 mins) was used to etch the outer 10-15 μm layer affected by α radiation and degrade each samples' feldspar content. During HF treatment, continuous magnetic stirring was used to effect isotropic etching of grains. 10% HCl was then added to remove acid soluble fluorides. Each sample was dried, resieved and quartz isolated from the remaining heavy mineral fraction using a sodium polytungstate density separation at 2.68g.cm^{-3}. Twelve 6 mm multi-grain aliquots (*c*. 3-6 mg) of quartz from each sample were then mounted on stainless steel cups for determination of D_e values.

All drying was conducted at 40°C to prevent thermal erosion of the signal. All acids and alkalis were Analar grade. All dilutions (removing toxic-corrosive and non-minerogenic luminescence-bearing substances) were conducted with distilled water to prevent signal contamination by extraneous particles.

3.0 Acquisition and accuracy of D_e value

All minerals naturally exhibit marked inter-sample variability in luminescence per unit dose (sensitivity). Therefore, the estimation of D_e acquired since burial requires calibration of the natural signal using known amounts of laboratory dose. D_e values were quantified using a single-aliquot regenerative-dose (SAR) protocol (Murray and Wintle 2000; 2003) facilitated by a Freiberg Instruments Lexsyg Smart irradiation-stimulation-detection system (Richter *et al*., 2015). Within this apparatus, optical signal stimulation is provided by an assembly of blue laser diodes, filtered to 445±3 nm conveying 50 using a 3 mm Schott GG420 and HC448/20 positioned in front of each laser diode. Infrared (IR) stimulation, provided by IR laser diodes stimulating at 850±3nm filtered by 3 mm RG 715 and delivering ~200 $mW.cm^{-2}$, was used to indicate the presence of contaminant feldspars (Hütt *et al*., 1988). Stimulated photon emissions from quartz aliquots are in the ultraviolet (UV) range. These were divided from stimulating photons by 2.5 mm Hoya U-340 glass filters, and a Delta BP 365/50 interference filter, then detected by a Hamamatsu UV-VIS (300-650 nm) bi-alkaline cathode photomultiplier. Aliquot irradiation was conducted using a 1.85 GBq $^{90}Sr/^{90}Y$ β source calibrated for multi-grain aliquots of 180-250 μm quartz against the 'Hotspot 800' ^{60}Co γ source located at the National Physical Laboratory (NPL), UK.

SAR by definition evaluates D_e through measuring the natural signal (Fig. 1) of a single aliquot and then regenerating that aliquot's signal by using known laboratory doses to enable calibration. For each aliquot, five different regenerative-doses were administered so as to image dose response. D_e values for each aliquot were then interpolated, and associated counting and fitting errors calculated, by way of exponential plus linear regression (Fig. 1). Weighted (geometric) mean D_e values were calculated from 12 aliquots using the central age model outlined by Galbraith *et al*. (1999) and are quoted at 1σ confidence (Table 1). The accuracy with which D_e equates to total absorbed dose and that dose absorbed since burial was assessed. The former can be considered a function of laboratory factors, the latter, one of environmental issues. Diagnostics were deployed to estimate the influence of these factors and criteria instituted to optimise the accuracy of D_e values.

3.1 Laboratory Factors

3.1.1 Feldspar contamination

The propensity of feldspar signals to fade and underestimate age, coupled with their higher sensitivity relative to quartz makes it imperative to quantify feldspar contamination. At room temperature, feldspars generate a signal (IRSL; Fig. 1) upon exposure to IR whereas quartz does not. The signal from feldspars contributing to OSL can be depleted by prior exposure to IR. For all aliquots the contribution of any remaining feldspars was estimated from the OSL IR depletion ratio (Duller, 2003). The influence of IR depletion on the OSL signal can be illustrated by comparing the regenerated post-IR OSL D_e with the applied regenerative-dose. If the addition to OSL by feldspars is insignificant, then the repeat dose ratio of OSL to post-IR OSL should be statistically consistent with unity (Table 1). If any aliquots do not fulfil this criterion, then the sample age estimate should be accepted tentatively. The source of feldspar contamination is rarely rooted in sample preparation; it predominantly results from the occurrence of feldspars as inclusions within quartz.

3.1.2 Preheating

Preheating aliquots between irradiation and optical stimulation is necessary to ensure comparability between natural and laboratory-induced signals. However, the multiple irradiation and preheating steps that are required to define single-aliquot regenerative-dose response leads to signal sensitisation, rendering calibration of the natural signal inaccurate. The SAR protocol (Murray and Wintle, 2000; 2003) enables this sensitisation to be monitored and corrected using a test dose, here set at 5 Gy preheated to 160°C for 10s, to track signal sensitivity between irradiation-preheat steps. However, the accuracy of sensitisation correction for both natural and laboratory signals can be preheat dependent.

The Dose Recovery test was used to assess the optimal preheat temperature for accurate correction and calibration of the time dependent signal. Dose Recovery (Fig. 2) attempts to quantify the combined effects of thermal transfer and

sensitisation on the natural signal, using a precise lab dose to simulate natural dose. The ratio between the applied dose and recovered D_e value should be statistically concordant with unity. For this diagnostic, 6 aliquots were each assigned a 10 s preheat between 140°C and 240°C.

That preheat treatment fulfilling the criterion of accuracy within the Dose Recovery test was selected to generate the final D_e value from a further 12 aliquots. Further thermal treatments, prescribed by Murray and Wintle (2000; 2003), were applied to optimise accuracy and precision. Optical stimulation occurred at 105ºC in order to minimise effects associated with photo-transferred thermoluminescence and maximise signal to noise ratios. Inter-cycle optical stimulation was conducted at 240ºC to minimise recuperation.

3.1.3 Irradiation

For all samples having D_e values in excess of 100 Gy, matters of signal saturation and laboratory irradiation effects are of concern. With regards the former, the rate of signal accumulation generally adheres to a saturating exponential form and it is this that limits the precision and accuracy of D_e values for samples having absorbed large doses. For such samples, the functional range of D_e interpolation by SAR has been verified up to 600 Gy by Pawley *et al*. (2010). Age estimates based on D_e values exceeding this value should be accepted tentatively.

3.1.4 Internal consistency

Abanico plots (Dietze *et al*., 2016) are used to illustrate inter-aliquot D_e variability (Fig. 3). D_e values are standardised relative to the central D_e value for natural signals and are described as overdispersed when >5% lie beyond $\pm 2\sigma$ of the standardising value; resulting from a heterogeneous absorption of burial dose and/or response to the SAR protocol. For multi-grain aliquots, overdispersion of natural signals does not necessarily imply inaccuracy. However where overdispersion is observed for regenerated signals, the efficacy of sensitivity correction may be problematic. Murray and Wintle (2000; 2003) suggest repeat dose ratios (Table 1) offer a measure of SAR protocol success, whereby ratios ranging across 0.9-1.1 represent effective sensitivity correction. However, this variation of repeat dose ratios in the high-dose region can have a significant impact on D_e interpolation.

3.2 Environmental factors

3.2.1 Incomplete zeroing

Post-burial OSL signals residual of pre-burial dose absorption can result where pre-burial sunlight exposure is limited in spectrum, intensity and/or period, leading to age overestimation. This effect is particularly acute for material eroded and redeposited sub-aqueously (Olley *et al*., 1998, 1999; Wallinga, 2002) and exposed to a burial dose of <20 Gy (e.g. Olley *et al*., 2004), has some influence in sub-aerial contexts but is rarely of consequence where aerial transport has occurred. Within single-aliquot regenerative-dose optical dating there are two diagnostics of partial resetting (or bleaching); signal analysis (Agersnap-Larsen *et al*., 2000; Bailey *et al*., 2003) and inter-aliquot D_e distribution studies (Murray *et al*., 1995).

Within this study, signal analysis was used to quantify the change in D_e value with respect to optical stimulation time for multi-grain aliquots. This exploits the existence of traps within minerogenic dosimeters that bleach with different efficiency for a given wavelength of light to verify partial bleaching. $D_e(t)$ plots (Fig. 4; Bailey *et al*., 2003) are constructed from separate integrals of signal decay as laboratory optical stimulation progresses. A statistically significant increase in natural $D_e(t)$ is indicative of partial bleaching assuming three conditions are fulfilled. Firstly, that a statistically significant increase in $D_e(t)$ is observed when partial bleaching is simulated within the laboratory. Secondly, that there is no significant rise in $D_e(t)$ when full bleaching is simulated. Finally, there should be no significant augmentation in $D_e(t)$ when zero dose is simulated. Where partial bleaching is detected, the age derived from the sample should be considered a maximum estimate only. However, the utility of signal analysis is strongly dependent upon a samples pre-burial experience of sunlight's spectrum and its residual to post-burial signal ratio. Given in the majority of cases, the spectral

exposure history of a deposit is uncertain, the absence of an increase in natural D_e (t) does not necessarily testify to the absence of partial bleaching.

Where requested and feasible, the insensitivities of multi-grain single-aliquot signal analysis may be circumvented by inter-aliquot D_e distribution studies. This analysis uses aliquots of single sand grains to quantify inter-grain D_e distribution. At present, it is contended that asymmetric inter-grain D_e distributions are symptomatic of partial bleaching and/or pedoturbation (Murray *et al*., 1995; Olley *et al*., 1999; Olley *et al*., 2004; Bateman *et al*., 2003). For partial bleaching at least, it is further contended that the D_e acquired during burial is located in the minimum region of such ranges. The mean and breadth of this minimum region is the subject of current debate, as it is additionally influenced by heterogeneity in microdosimetry, variable inter-grain response to SAR and residual to post-burial signal ratios.

3.2.2 Turbation

As noted in section 3.1.1, the accuracy of sedimentation ages can further be controlled by post-burial trans-strata grain movements forced by pedo- or cryoturbation. Berger (2003) contends pedogenesis prompts a reduction in the apparent sedimentation age of parent material through bioturbation and illuviation of younger material from above and/or by biological recycling and resetting of the datable signal of surface material. Berger (2003) proposes that the chronological products of this remobilisation are A-horizon age estimates reflecting the cessation of pedogenic activity, Bc/C-horizon ages delimiting the maximum age for the initiation of pedogenesis with estimates obtained from Bt-horizons providing an intermediate age 'close to the age of cessation of soil development'. Singhvi et al. (2001), in contrast, suggest that B and C-horizons closely approximate the age of the parent material, the A-horizon, that of the 'soil forming episode'. Recent analyses of inter-aliquot D_e distributions have reinforced this complexity of interpreting burial age from pedoturbated deposits (Lombard *et al*., 2011; Gliganic *et al*., 2015; Jacobs *et al*., 2008; Bateman *et al*., 2007; Gliganic *et al*., 2016). At present there is no definitive post-sampling mechanism for the direct detection of and correction for post-burial sediment remobilisation. However, intervals of palaeosol evolution can be delimited by a maximum age derived from parent material and a minimum age obtained from a unit overlying the palaeosol. Inaccuracy forced by cryoturbation may be bidirectional, heaving older material upwards or drawing younger material downwards into the level to be dated. Cryogenic deformation of matrix-supported material is, typically, visible; sampling of such cryogenically-disturbed sediments can be avoided.

4.0 Acquisition and accuracy of D_r value

Lithogenic D_r values were defined through measurement of U, Th and K radionuclide concentration and conversion of these quantities into β and γ D_r values (Table 1). β contributions were estimated from sub-samples by laboratory-based γ spectrometry using an Ortec GEM-S high purity Ge coaxial detector system, calibrated using certified reference materials supplied by CANMET. γ dose rates can be estimated from *in situ* NaI gamma spectrometry or, where direct measurements are unavailable as in the present case, from laboratory-based Ge γ spectrometry. *In situ* measurements reduce uncertainty relating to potential heterogeneity in the γ dose field surrounding each sample. The level of U disequilibrium was estimated by laboratory-based Ge γ spectrometry. Estimates of radionuclide concentration were converted into D_r values (Adamiec and Aitken, 1998), accounting for D_r modulation forced by grain size (Mejdahl, 1979) and present moisture content (Zimmerman, 1971). Cosmogenic D_r values were calculated on the basis of sample depth, geographical position and matrix density (Prescott and Hutton, 1994).

The spatiotemporal validity of D_r values can be considered a function of five variables. Firstly, age estimates devoid of *in situ* γ spectrometry data should be accepted tentatively if the sampled unit is heterogeneous in texture or if the sample is located within 300 mm of strata consisting of differing texture and/or mineralogy. However, where samples are obtained throughout a vertical profile, consistent values of γ D_r based solely on laboratory measurements may evidence the

homogeneity of the γ field and hence accuracy of γ D_r values. Secondly, disequilibrium can force temporal instability in U and Th emissions. The impact of this infrequent phenomenon (Olley *et al*., 1996) upon age estimates is usually insignificant given their associated margins of error. However, for samples where this effect is pronounced (>50% disequilibrium between ^{238}U and ^{226}Ra; Fig. 5), the resulting age estimates should be accepted tentatively. Thirdly, pedogenically-induced variations in matrix composition of B and C-horizons, such as radionuclide and/or mineral remobilisation, may alter the rate of energy emission and/or absorption. If D_r is invariant through a dated profile and samples encompass primary parent material, then element mobility is likely limited in effect. Fourthly, spatiotemporal detractions from present moisture content are difficult to assess directly, requiring knowledge of the magnitude and timing of differing contents. However, the maximum influence of moisture content variations can be delimited by recalculating D_r for minimum (zero) and maximum (saturation) content. Finally, temporal alteration in the thickness of overburden alters cosmic D_r values. Cosmic D_r often forms a negligible portion of total D_r. It is possible to quantify the maximum influence of overburden flux by recalculating D_r for minimum (zero) and maximum (surface sample) cosmic D_r.

5.0 Estimation of Age

Ages reported in Table 1 provide an estimate of sediment burial period based on mean D_e and D_r values and their associated analytical uncertainties. Uncertainty in age estimates is reported as a product of systematic and experimental errors, with the magnitude of experimental errors alone shown in parenthesis (Table 1). Cumulative frequency plots indicate the inter-aliquot variability in age (Fig. 6). The maximum influence of temporal variations in D_r forced by minima-maxima in moisture content and overburden thickness is also illustrated in Fig. 6. Where uncertainty in these parameters exists this age range may prove instructive, however the combined extremes represented should not be construed as preferred age estimates. The analytical validity of each sample is presented in Table 2.

6.0 Analytical uncertainty

All errors are based upon analytical uncertainty and quoted at 1σ confidence. Error calculations account for the propagation of systematic and/or experimental (random) errors associated with D_e and D_r values.

For D_e values, systematic errors are confined to laboratory β source calibration. Uncertainty in this respect is that combined from the delivery of the calibrating γ dose (1.2%; NPL, pers. comm.), the conversion of this dose for SiO_2 using the respective mass energy-absorption coefficient (2%; Hubbell, 1982) and experimental error, totalling 3.5%. Mass attenuation and bremsstrahlung losses during γ dose delivery are considered negligible. Experimental errors relate to D_e interpolation using sensitisation corrected dose responses. Natural and regenerated sensitisation corrected dose points (S_i) were quantified by,

$$S_i = (D_i - x.L_i) / (d_i - x.L_i) \qquad \textbf{Eq.1}$$

where D_i = Natural or regenerated OSL, initial 0.2 s
L_i = Background natural or regenerated OSL, final 5 s
d_i = Test dose OSL, initial 0.2 s
x = Scaling factor, 0.08

The error on each signal parameter is based on counting statistics, reflected by the square-root of measured values. The propagation of these errors within Eq. 1 generating σS_i follows the general formula given in Eq. 2. σS_i were then used to define fitting and interpolation errors within exponential plus linear regressions.

For D_r values, systematic errors accommodate uncertainty in radionuclide conversion factors (5%), β attenuation coefficients (5%), matrix density (0.20 $g.cm^{-3}$), vertical thickness of sampled section (specific to sample collection device), saturation moisture content (3%), moisture content attenuation (2%) and burial moisture content (25% relative, unless direct evidence exists of the magnitude and period of differing content). Experimental errors are associated with radionuclide quantification for each sample by Ge gamma spectrometry.

The propagation of these errors through to age calculation was quantified using the expression,

$$\sigma y\ (\delta y/\delta x) = (\Sigma\ ((\delta y/\delta x_n).\sigma x_n)^2)^{1/2} \qquad \textbf{Eq. 2}$$

where y is a value equivalent to that function comprising terms x_n and where σy and σx_n are associated uncertainties.

Errors on age estimates are presented as combined systematic and experimental errors and experimental errors alone. The former (combined) error should be considered when comparing luminescence ages herein with independent chronometric controls. The latter assumes systematic errors are common to luminescence age estimates generated by means identical to those detailed herein and enable direct comparison with those estimates.

Fig. 1 Signal Calibration

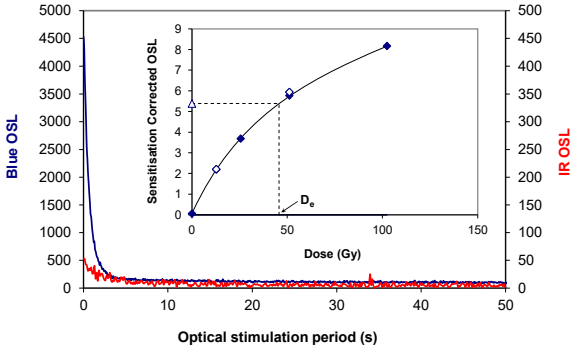

Fig. 2 Dose Recovery

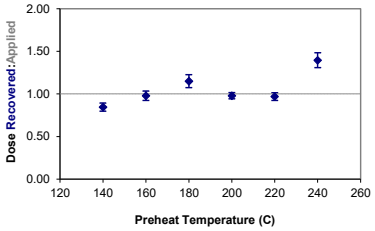

Fig. 4 Signal Analysis

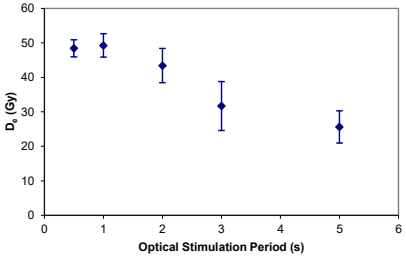

Fig. 3 Inter-aliquot D_e distribution

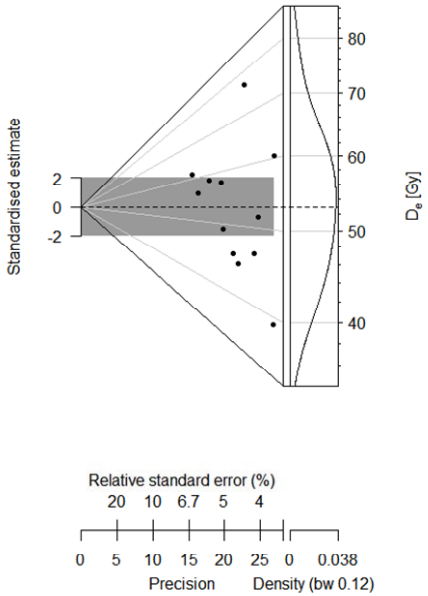

Fig. 5 U Decay Activity

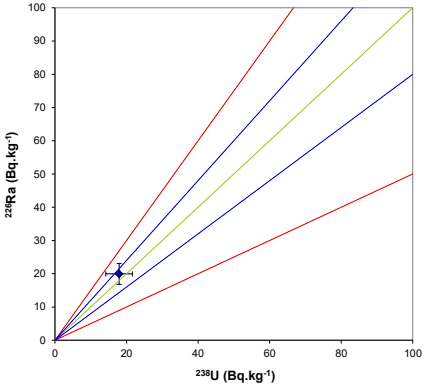

Fig. 6 Age Range

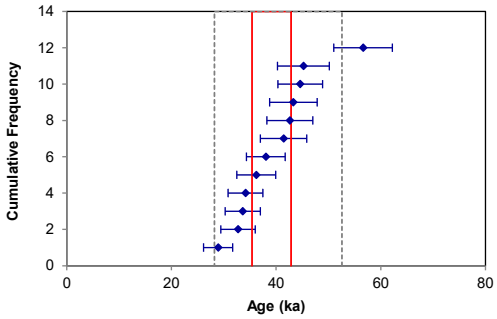

Fig. 1 Signal Calibration Natural blue and laboratory-induced infrared (IR) OSL signals. Detectable IR signal decays are diagnostic of feldspar contamination. Inset, the natural blue OSL signal (open triangle) of each aliquot is calibrated against known laboratory doses to yield equivalent dose (D_e) values. Repeats of low and high doses (open diamonds) illustrate the success of sensitivity correction.

Fig. 2 Dose Recovery The acquisition of D_e values is necessarily predicated upon thermal treatment of aliquots succeeding environmental and laboratory irradiation. The Dose Recovery test quantifies the combined effects of thermal transfer and sensitisation on the natural signal using a precise lab dose to simulate natural dose. Based on this an appropriate thermal treatment is selected to generate the final D_e value.

Fig. 3 Inter-aliquot D_e distribution Abanico plot of inter-aliquot statistical concordance in D_e values derived from **natural** irradiation. Discordant data (those points lying beyond **±2 standardised ln D_e**) reflect heterogeneous dose absorption and/or inaccuracies in calibration.

Fig. 4 Signal Analysis Statistically significant increase in **natural** D_e value with signal stimulation period is indicative of a partially-bleached signal, provided a significant increase in D_e results from **simulated partial bleaching** followed by insignificant adjustment in D_e for simulated **zero** and **full bleach** conditions. Ages from such samples are considered maximum estimates. In the absence of a significant rise in D_e with stimulation time, simulated partial bleaching and zero/full bleach tests are not assessed.

Fig. 5 U Activity Statistical concordance (equilibrium) in the activities of the daughter radioisotope ^{226}Ra with its parent ^{238}U may signify the temporal stability of D_r emissions from these chains. Significant differences (disequilibrium; >50%) in activity indicate addition or removal of isotopes creating a time-dependent shift in D_r values and increased uncertainty in the accuracy of age estimates. A 20% disequilibrium marker is also shown.

Fig. 6 Age Range The Cumulative frequency plot indicates the inter-aliquot variability in age. It also shows the **mean age range**; an estimate of sediment burial period based on mean D_e and D_r values with associated analytical uncertainties. The **maximum influence** of temporal variations in D_r forced by minima-maxima variation in moisture content and overburden thickness is outlined and may prove instructive where there is uncertainty in these parameters. However the combined extremes represented should not be construed as preferred age estimates.

Sample: GL21068

Fig. 1 Signal Calibration

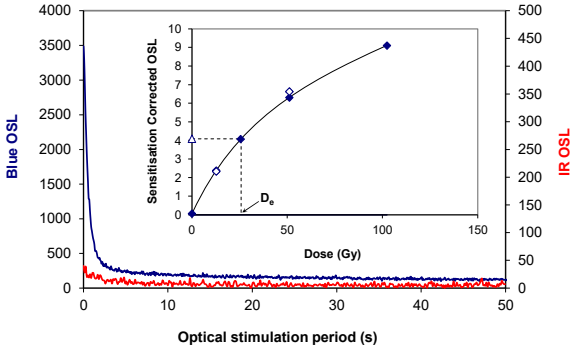

Fig. 2 Dose Recovery

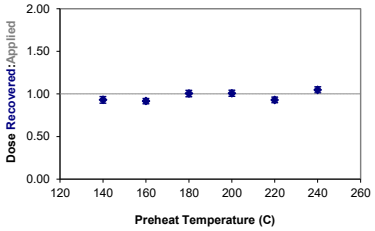

Fig. 4 Signal Analysis

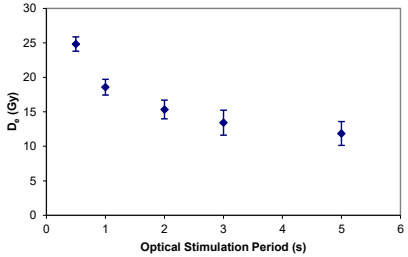

Fig. 3 Inter-aliquot D_e distribution

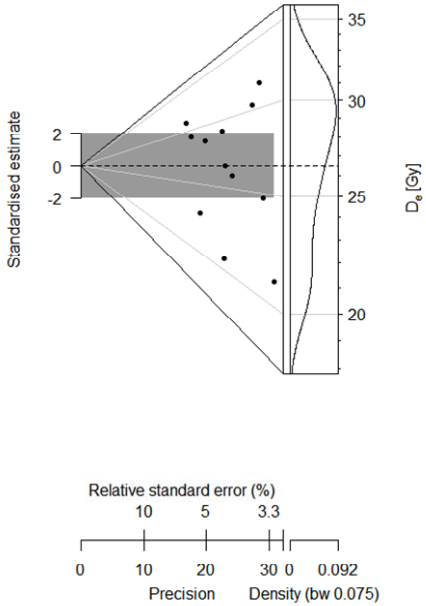

Fig. 5 U Decay Activity

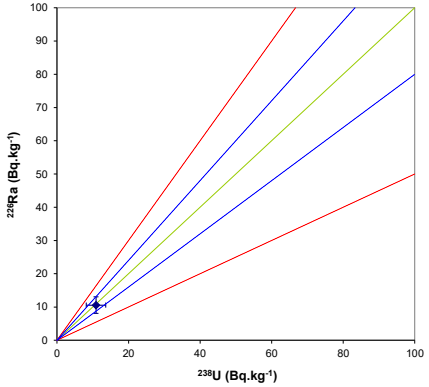

Fig. 6 Age Range

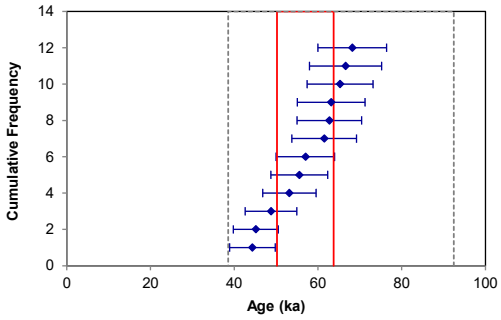

Fig. 1 Signal Calibration Natural blue and laboratory-induced infrared (IR) OSL signals. Detectable IR signal decays are diagnostic of feldspar contamination. Inset, the natural blue OSL signal (open triangle) of each aliquot is calibrated against known laboratory doses to yield equivalent dose (D_e) values. Repeats of low and high doses (open diamonds) illustrate the success of sensitivity correction.

Fig. 2 Dose Recovery The acquisition of D_e values is necessarily predicated upon thermal treatment of aliquots succeeding environmental and laboratory irradiation. The Dose Recovery test quantifies the combined effects of thermal transfer and sensitisation on the natural signal using a precise lab dose to simulate natural dose. Based on this an appropriate thermal treatment is selected to generate the final D_e value.

Fig. 3 Inter-aliquot D_e distribution Abanico plot of inter-aliquot statistical concordance in D_e values derived from **natural** irradiation. Discordant data (those points lying beyond **±2 standardised ln D_e**) reflect heterogeneous dose absorption and/or inaccuracies in calibration.

Fig. 4 Signal Analysis Statistically significant increase in **natural** D_e value with signal stimulation period is indicative of a partially-bleached signal, provided a significant increase in D_e results from **simulated partial bleaching** followed by insignificant adjustment in D_e for simulated **zero** and **full bleach** conditions. Ages from such samples are considered maximum estimates. In the absence of a significant rise in D_e with stimulation time, simulated partial bleaching and zero/full bleach tests are not assessed.

Fig. 5 U Activity Statistical concordance (equilibrium) in the activities of the daughter radioisotope ^{226}Ra with its parent ^{238}U may signify the temporal stability of D_r emissions from these chains. Significant differences (disequilibrium; >50%) in activity indicate addition or removal of isotopes creating a time-dependent shift in D_r values and increased uncertainty in the accuracy of age estimates. A 20% disequilibrium marker is also shown.

Fig. 6 Age Range The Cumulative frequency plot indicates the inter-aliquot variability in age. It also shows the **mean age range**; an estimate of sediment burial period based on mean D_e and D_r values with associated analytical uncertainties. The **maximum influence** of temporal variations in D_r forced by minima-maxima variation in moisture content and overburden thickness is outlined and may prove instructive where there is uncertainty in these parameters. However the combined extremes represented should not be construed as preferred age estimates.

Sample: GL21069

References

Adamiec, G. and Aitken, M.J. (1998) Dose-rate conversion factors: new data. *Ancient TL*, 16, 37-50.

Agersnap-Larsen, N., Bulur, E., Bøtter-Jensen, L. and McKeever, S.W.S. (2000) Use of the LM-OSL technique for the detection of partial bleaching in quartz. *Radiation Measurements*, 32, 419-425.

Aitken, M. J. (1998) An introduction to optical dating: the dating of Quaternary sediments by the use of photon-stimulated luminescence. Oxford University Press.

Bailey, R.M., Singarayer, J.S. , Ward, S. and Stokes, S. (2003) Identification of partial resetting using D_e as a function of illumination time. *Radiation Measurements*, 37, 511-518.

Bateman, M.D., Frederick, C.D., Jaiswal, M.K., Singhvi, A.K. (2003) Investigations into the potential effects of pedoturbation on luminescence dating. *Quaternary Science Reviews*, 22, 1169-1176.

Bateman, M.D., Boulter, C.H., Carr, A.S., Frederick, C.D., Peter, D. and Wilder, M. (2007) Detecting post-depositional sediment disturbance in sandy deposits using optical luminescence. *Quaternary Geochronology*, 2, 57-64.

Berger, G.W. (2003). Luminescence chronology of late Pleistocene loess-paleosol and tephra sequences near Fairbanks, Alaska. *Quaternary Research*, 60, 70-83.

Bøtter-Jensen, L., McKeever, S.W.S. and Wintle, A.G. (2003) Optically Stimulated Luminescence Dosimetry. Elsevier, Amsterdam.

Dietze, M., Kreutzer, S., Burow, C., Fuchs, M.C., Fischer, M., Schmidt, C. (2016) The abanico plot: visualising chronometric data with individual standard errors. *Quaternary Geochronology*, 31, 1-7.

Duller, G.A.T (2003) Distinguishing quartz and feldspar in single grain luminescence measurements. *Radiation Measurements*, 37, 161-165.

Galbraith, R. F., Roberts, R. G., Laslett, G. M., Yoshida, H. and Olley, J. M. (1999) Optical dating of single and multiple grains of quartz from Jinmium rock shelter (northern Australia): Part I, Experimental design and statistical models. *Archaeometry*, 41, 339-364.

Gliganic, L.A., May, J.-H. and Cohen, T.J. (2015). All mixed up: using single-grain equivalent dose distributions to identify phases of pedogenic mixing on a dryland alluvial fan. *Quaternary International*, 362, 23-33.

Gliganic, L.A., Cohen, T.J., Slack, M. and Feathers, J.K. (2016) Sediment mixing in Aeolian sandsheets identified and quantified using single-grain optically stimulated luminescence. *Quaternary Geochronology*, 32, 53-66.

Huntley, D.J., Godfrey-Smith, D.I. and Thewalt, M.L.W. (1985) Optical dating of sediments. *Nature*, 313, 105-107.

Hubbell, J.H. (1982) Photon mass attenuation and energy-absorption coefficients from 1keV to 20MeV. *International Journal of Applied Radioisotopes*, 33, 1269-1290.

Hütt, G., Jaek, I. and Tchonka, J. (1988) Optical dating: K-feldspars optical response stimulation spectra. *Quaternary Science Reviews*, 7, 381-386.

Jacobs, A., Wintle, A.G., Duller, G.A.T, Roberts, R.G. and Wadley, L. (2008) New ages for the post-Howiesons Poort, late and finale middle stone age at Sibdu, South Africa. *Journal of Archaeological Science*, 35, 1790-1807.

Lombard, M., Wadley, L., Jacobs, Z., Mohapi, M. and Roberts, R.G. (2011) Still Bay and serrated points from the Umhlatuzana rock shelter, Kwazulu-Natal, South Africa. *Journal of Archaeological Science*, 37, 1773-1784.

Mejdahl, V. (1979) Thermoluminescence dating: beta-dose attenuation in quartz grains. *Archaeometry*, 21, 61-72.

Murray, A.S. and Olley, J.M. (2002) Precision and accuracy in the Optically Stimulated Luminescence dating of sedimentary quartz: a status review. *Geochronometria*, 21, 1-16.

Murray, A.S. and Wintle, A.G. (2000) Luminescence dating of quartz using an improved single-aliquot regenerative-dose protocol. *Radiation Measurements*, 32, 57-73.

Murray, A.S. and Wintle, A.G. (2003) The single aliquot regenerative dose protocol: potential for improvements in reliability. *Radiation Measurements*, 37, 377-381.

Murray, A.S., Olley, J.M. and Caitcheon, G.G. (1995) Measurement of equivalent doses in quartz from contemporary water-lain sediments using optically stimulated luminescence. *Quaternary Science Reviews*, 14, 365-371.

Olley, J.M., Murray, A.S. and Roberts, R.G. (1996) The effects of disequilibria in the Uranium and Thorium decay chains on burial dose rates in fluvial sediments. *Quaternary Science Reviews*, 15, 751-760.

Olley, J.M., Caitcheon, G.G. and Murray, A.S. (1998) The distribution of apparent dose as determined by optically stimulated luminescence in small aliquots of fluvial quartz: implications for dating young sediments. *Quaternary Science Reviews*, 17, 1033-1040.

Olley, J.M., Caitcheon, G.G. and Roberts R.G. (1999) The origin of dose distributions in fluvial sediments, and the prospect of dating single grains from fluvial deposits using -optically stimulated luminescence. *Radiation Measurements,* 30, 207-217.

Olley, J.M., Pietsch, T. and Roberts, R.G. (2004) Optical dating of Holocene sediments from a variety of geomorphic settings using single grains of quartz. *Geomorphology*, 60, 337-358.

Pawley, S.M., Toms, P.S., Armitage, S.J., Rose, J. (2010) Quartz luminescence dating of Anglian Stage fluvial sediments: Comparison of SAR age estimates to the terrace chronology of the Middle Thames valley, UK. *Quaternary Geochronology*, 5, 569-582.

Prescott, J.R. and Hutton, J.T. (1994) Cosmic ray contributions to dose rates for luminescence and ESR dating: large depths and long-term time variations. *Radiation Measurements*, 23, 497-500.

Richter, D., Richter, A. and Dornich, K. (2015) Lexsyg Smart – a Luminescence detection system for dosimetry, material research and dating application. *Geochronometria*, 42, 202-209.

Singhvi, A.K., Bluszcz, A.., Bateman, M.D., Someshwar Rao, M. (2001). Luminescence dating of loess-palaeosol sequences and coversands: methodological aspects and palaeoclimatic implications. *Earth Science Reviews*, 54, 193-211.

Smith, B.W., Rhodes, E.J., Stokes, S., Spooner, N.A. (1990) The optical dating of sediments using quartz. *Radiation Protection Dosimetry*, 34, 75-78.

Spooner, N.A. (1993) The validity of optical dating based on feldspar. Unpublished D.Phil. thesis, Oxford University.

Templer, R.H. (1985) The removal of anomalous fading in zircons. *Nuclear Tracks and Radiation Measurements*, 10, 531-537.

Wallinga, J. (2002) Optically stimulated luminescence dating of fluvial deposits: a review. *Boreas* 31, 303-322.

Wintle, A.G. (1973) Anomalous fading of thermoluminescence in mineral samples. *Nature*, 245, 143-144.

Zimmerman, D. W. (1971) Thermoluminescent dating using fine grains from pottery. *Archaeometry*, 13, 29-52.